Grosmougin *et al. BMC Ecology and Evolution* (2025) 25:65
https://doi.org/10.1186/s12862-025-02397-5

BMC Ecology and Evolution

RESEARCH **Open Access**

Forelimb feathering, soft tissues, and skeleton of the flying dromaeosaurid *Microraptor*

Maxime Grosmougin[1], Xiaoli Wang[2,3*], Xiaoting Zheng[2,3*], Thomas G. Kaye[4], Matthieu Chotard[1], Luke A. Barlow[1], T. Alexander Deccechi[5], Michael B. Habib[6], Juned Zariwala[7], Scott A. Hartman[8], Xing Xu[9,10] and Michael Pittman[1*]

Abstract

Background *Microraptor* is an essential animal for understanding the evolution of flight in birds and their closest relatives. Recent studies have uncovered evidence of its powered flight potential and details of its diet and ecology. However, we are still missing a thorough description of the anatomy of *Microraptor* connecting feathers, soft tissues, and osteology together. Here we focus on the forelimbs of ten new *Microraptor* specimens from the Shandong Tianyu Museum of Nature studied under Laser-Stimulated Fluorescence. We compared our results with extensively studied existing specimens (e.g., IVPP V13352 and BMNHC PH881), other key early paravians (e.g., *Anchiornis*, *Archaeopteryx* and *Confuciusornis*), as well as modern birds to expand what we know about flight origins, and early diverging paravian theropods more generally.

Results Plumage was previously only minimally known. Reconstruction of the forewings relied on brief descriptions of the primary and secondary feathers. With the new specimens studied here, we uncovered the whole shape of the wing from the tip of the digits to the proximal end of the ulna, the different layers of feathers, and the number as well as characteristics of each feather type. Skeletal features of the forelimb remain mostly unchanged from previous descriptions, but we bring new information regarding wrist bones and functional implications of humerus and radius features. The most significant advances have been recovered in preserved soft tissues including those of the shoulder, propatagium and postpatagium. In particular, the new specimens of *Microraptor* help us to understand the impact of the soft tissues on lift generation and cohesiveness of the forewing.

Conclusions This study permitted us to recreate the most accurate forewing of *Microraptor* to date. Taken together, new information on the forelimb anatomy shows that *Microraptor* shares many of the forewing characteristics of early avialans and modern birds, and helps us to better understand the flight behaviour and ecology of this iconic and unique 'four-winged' animal along with its role in flight evolution. These results serve as a starting point to conduct more precise and integrative analyses (e.g., including hindwings and/or tail) on the locomotor behaviours of *Microraptor*.

Keywords *Microraptor*, Theropod, Feathered dinosaur, Flight anatomy, Forelimb, Wing, Feathering, Flight evolution

*Correspondence:
Xiaoli Wang
wang_7355@163.com
Xiaoting Zheng
ty4291666@163.com
Michael Pittman
mpittman@cuhk.edu.hk
Full list of author information is available at the end of the article

Background

Modern birds have a myriad of different wing feathering patterns, wing shapes and locomotor behaviours. Wing shape is one of the main parameters influencing aerodynamic performance in modern birds [1], as it is the primary surface that interacts with the airflow. Although there seems to be a better correlation between the locomotor behaviour of modern birds and other parameters such as the range of motion of the wing [2], wing shape can provide preliminary and basic information about flight capabilities.

Whereas wing feather arrangement and morphology are more widely discussed (e.g., Longrich et al. [3], Saitta et al. [4], Lefèvre et al. [5] and O'Connor [6]), the wing shape of early paravians has rarely been compared to the wing shape of modern birds, even though some of the best specimens from the Jehol Biota and of *Archaeopteryx* preserve extensive feathering. In order to reconstruct the wing shape of these animals, much care must be taken to assess the degree of folding of the wing, which can easily hide underlying feathers, as well as the layering, displacement and preservation of feathers. However, even with the complete reconstruction of the wing shape, such comparisons are not straightforward as some wing features that have no modern analogues need to be analysed especially carefully [7]. For example, the wing of the early pygostylian bird *Confuciusornis*, with extremely long primary feathers compared to its secondary feathers, seems to have no modern analogue [8]. Several early diverging paravians, including *Microraptor*, also have elongated hindlimb feathers potentially linked to flight as part of a 'four-winged' condition, which is different from the 'two-winged' condition of today's birds [9]. Further study of early paravian wing shape is needed to evaluate the significance of these early body plans and to reconstruct the shape of ancestral wings in order to better understand the origin and evolution of modern wing shapes.

Using specimen BMNHC PH881, the skeletal anatomy of *Microraptor* was thoroughly described by Pei et al. [10] and its feathering was reconstructed by Li et al. [11] using knowledge of the primary remiges and secondary feathers, and traces of the secondary coverts. New studies on the soft tissues of the forewing of *Microraptor* have brought insight into its upstroke capabilities [12]. However, we are still lacking evidence on the type and arrangement of feathers across the entire forewing of *Microraptor*, which is needed to better evaluate the aerodynamic performance of this dromaeosaurid, especially when *Microraptor* has been a key paravian in the investigation of theropod flight evolution [13–16].

In order to address these gaps, we restudied four key *Microraptor* specimens that are used in current reconstructions of locomotor ecology and models, and described ten new *Microraptor* specimens from the Shandong Tianyu Museum of Nature that record novel aspects of the forewing anatomy. We compared the forewing anatomy of *Microraptor* with early diverging paravians and with modern birds. Our goals are to 1) provide a more accurate reconstruction of the forewing feathering of *Microraptor*, particularly by adding information from previously undescribed feathers, 2) identify skeletal features that could give new insights into the flight capabilities of *Microraptor*, and 3) describe new soft tissues revealed by Laser-Stimulated Fluorescence (LSF) and comment on their role in how *Microraptor* used its forewing. This new information helped us to reconstruct the most accurate model of an early paravian wing to date. Our study demonstrates the importance of studying new specimens bearing different anatomical information to improve our reconstructions and our understanding of the palaeoecology and evolutionary history of feathered dinosaurs.

Institutional abbreviations

BMNHC, Beijing Museum of Natural History Collections, Beijing, China (renamed as National Natural History Museum of China, NNHMC); HMN, Museum für Naturkunde, Berlin, Germany; IVPP, Institute for Vertebrate Paleontology and Paleoanthropology, Beijing, China; PMoL, Paleontological Museum of Liaoning, Shenyang, Liaoning, China; PSM, Puget Sound Museum, University of Puget Sound Collins Memorial Library, Tacoma, Washington, United States of America; STM, Shandong Tianyu Museum of Nature, Pingyi, Shandong, China; WDC, Wyoming Dinosaur Center, Thermopolis, Wyoming, United States of America.

Methods

Materials

The specimen sample of our study comprises published specimens IVPP V12230, V13352 and V13320 as well as BMNHC PH881, and new specimens STM 5–4, 5–5, 5–9, 5–75, 5–93, 5–109, 5–142, 5–150, 5–172, and 5–221. All specimens were collected from the Lower Cretaceous Jehol Group of northeastern China and are housed in permanent repositories accessible to researchers with visit authorisations (Institute of Vertebrate Paleontology and Paleoanthropology, National Natural History Museum of China formerly the Beijing Museum of Natural History, and Shandong Tianyu Museum of Nature) [17]. The new specimens were all assigned to the subfamily Microraptorinae based on different combinations of the following characters (see Table S1 in Additional file 1 for the detail of each specimen): large supracoracoid fenestra; combined length of metacarpal I and phalanx

I-1 shorter than that of metacarpal II; prominent lateral tubercle on the pubic shaft; subarctometatarsalian pes [18]; narrow-waisted coracoid; dorsally situated articular surface on manus unguals; pelvis opisthopubic with boot bent sharply backwards; postacetabular ilium bent sharply ventrally; nearly vertical ischium with enlarged obturator process; femur with elevated head (above greater trochanter); metatarsal I more distally situated than other known dromaeosaurids (corrected from proximally to distally *contra* Gong et al. [19]); metatarsal V over 50% length of metatarsal IV [19]; semilunate distal carpal that is small and covers about half the base of metacarpals I and II; combined length of metacarpal I plus phalanx I-1 is equal to or less than the length of metacarpal II; caudal chevrons have very elongated posterior extensions [20]. The specimens can be further referred to the genus *Microraptor* based on different combinations of the following characters (see Table S1 in Additional file 1 for the detail of each specimen): extremely slender manual phalanx III-3, dorsoventral thickness of its midshaft is about 1/3 to 1/2 lateral width of phalanx III-1; length ratio of manual phalanx III-1 to II-1 is close to 0.8; slender ischium in lateral view, anteroposterior width of the distal end is about 40% of the proximodistal length along the posterior margin [18]; metacarpal III smaller than metacarpal II; extremely short manual phalanx III-2 that is less than one quarter of the length of manual III-1; manual III-3 shorter than III-1 with the small distal articulation of manual III-3 skewed ventrally [21]; skull lacks the surface ornamentation of *Sinornithosaurus* and a subfenestral fossa [22]. We did not identify the specimens to the species level as there is still controversy regarding the diagnoses and interrelationships among the different *Microraptor* species *M. zhaoianus*, *M. gui* and *M. hanquigi*; which could be synonymous [10, 18, 20, 23, 24].

Articulated and disarticulated feathers of modern birds sampling the morphologic and phylogenetic breadth of the group were studied and accessed online through Featherbase [25], the atlas of avian feathers, Vogelfedern [26], the Puget Sound Museum Wing and Tails Image Collection [27], and on the Cornell College of Agriculture and Life Science (CALS) website [28]. Feathers are named because of their anatomical positioning. Functional implications are discussed explicitly as modern feather form-function relationships are not presumed. For the comparative data of feather curvature, we used a subset of specimens that had complete disarticulated primary remex series available from these sources and had diverse locomotor behaviours: *Columba livia* #155, *Ara ararauna* #190, *Tichodroma muraria* #1000, *Falco peregrinus* #1698, *Phoebastria immutabilis* #2091, *Strix aluco* #2145, *Anas plathyrhynchos* #2299, *Colibri coruscans* #2722, *Accipiter nisus* #3532 (Featherbase), *Gallus gallus* (Vogelfedern), and *Gymnogyps californianus* (Cornell CALS website). For skeletal data of modern birds, we used a morphologically and phylogenetically diverse range of 40 digitalised skeletal specimens accessed online through the website of the Smithsonian Institution, National Museum of Natural History, Collection of Birds [29]: see Table S2 in Additional file 1 for collection numbers. *Microraptor* specimens were compared to a range of early diverging paravian specimens including *Archaeopteryx* (HMN 1880, WDC-CGS-100, and 11th specimen), *Anchiornis* (STM 0–114, 0–118, 0–127, 0–132, 0–133, 0–144 and 0–147) and *Confuciusornis* (STM 13–12, 13–45, 13–54 and 13–160) with the help of new white light and Laser-Stimulated Fluorescence images. Available images of published specimens of the study taxa were also used.

Laser-Stimulated Fluorescence

All specimens were studied under white light (WL) and Laser-Stimulated Fluorescence (LSF), except for specimen BMNHC PH881 which was only observed under WL. LSF imaging is based on the original protocol of Kaye et al. [30], which has previously been used to study the bones, feathers and soft tissues of several feathered dinosaurs including *Microraptor* [8, 12, 31–34]. A 0.5 W 405-nm laser diode was used to fluoresce the fossil specimens according to standard laser safety protocol. Thirty-second time-exposed images were taken with a Nikon D810 DSLR camera fitted with a 425-nm laser-blocking filter. Postprocessing was applied uniformly across entire images (equalisation, saturation, and colour balance) in graphics software Photoshop CS6.

Comparative methods

We compared *Microraptor* specimens' osteology, feathers and soft tissues with closely related early diverging paravians, especially *Anchiornis*, *Archaeopteryx* and *Confuciusornis*, and modern birds. Measurements of bone and feather lengths as well as the number of preserved feathers by feather type of each *Microraptor* specimen are compiled in Table S3 of Additional file 1. To be consistent with existing dromaeosaurid literature, this study uses the traditional numbers I-II-III for the metacarpals (Mc) and manual digits. This choice should not be assumed to reflect our views on the homology of the manual digits, which is still open to debate [35–37]. Measurements of the manual claws are done using the outer angle of the ungual and sheath following the method of Pike and Maitland [38].

The structure and morphology of feathers can be highly impacted by taphonomic processes, potentially leading to misinterpretation [39]. To minimise these issues, we studied a broad sample of specimens and analysed a

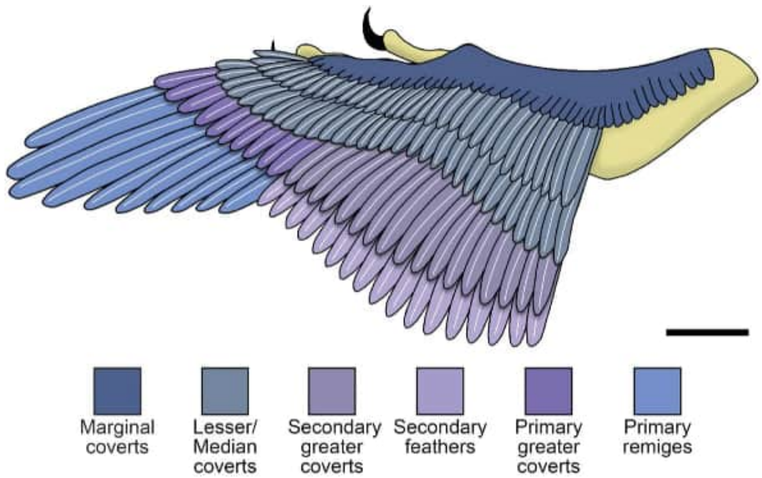

Fig. 1 Composite reconstruction of the forewing feathering of *Microraptor* based on 14 studied specimens. The wing has four to five layers of feathers: one of marginal coverts, possibly one of lesser coverts, one of ~35 median coverts, one of greater coverts (~ 10 primary coverts and ~17 secondary coverts) and one of flight feathers (~ 10 primary remiges plus ~17 secondary feathers). Secondary greater covert rachises are directly located on top of the secondary feather rachises, whereas the rachises of primary greater coverts are located offset compared to primary remex rachises, as seen in modern birds. Marginal coverts of *Microraptor* follow the same pattern as seen in modern birds. Scale bar is 50 mm

variety of feathers in each specimen to assess the possible taphonomic deformation in our measurements of the feathers as preserved. Feathers are labelled according to the numbering convention of modern birds: feathers of the manus are numbered from proximal to distal, and feathers of the forearm are numbered from distal to proximal [40, 41]. Median and lesser coverts are labelled marginal coverts in some cases. In this study, we label covert feathers preserved within the wing plane and shorter than greater coverts as median primary/secondary coverts and as lesser primary/secondary coverts. Marginal coverts are often displaced and preserved anteriorly from the manus and ulna in *Microraptor* specimens. Projections of the feathers from the bones of *Microraptor* specimens were measured with the proximal end of the bone as the 0° reference and the distal end of the bone as the 180° reference. The curvature of the feather is obtained by measuring the angle between the line following the straight portion of the rachis and the line connecting the apex of the feather and the tangent point where the rachis deviates from the first line.

Body mass estimates are obtained using the method from Benson et al. [42]. The femur lengths of the specimens were used to estimate their femur circumference. Circumference was then used as a proxy for body mass estimates as suggested by Campione et al. [43]. Femur circumferences were estimated from femur length because specimens are embedded and damage/compression of femur shafts make measurements of the shaft radius complex. Although our mass estimates of the four published specimens are slightly different from previous studies (see Turner et al. [44], Allen et al. [45], and Dececchi et al. [46]), this method gives mass estimates that can be compared between each other and identify potential intrageneric and/or ontogenetic variation in the *Microraptor* specimens we studied (see Chotard et al. [47] for more detail).

Results

Microraptor forelimb feathering

Laser-Stimulated Fluorescence of new and existing *Microraptor* specimens reveals otherwise hidden feather details, permitting the description of new records of feather types from the genus: primary and secondary greater coverts, median coverts, lesser coverts, and marginal coverts. Coverts have been mentioned in previous studies of *Microraptor* [3, 11, 21], but this is the first time that the coverts have been distinguished into primary greater, secondary greater, median, and lesser coverts. The new specimens also bring insight into the forewing shape of *Microraptor* by preserving feathering from the ulna to the tip of the manus. Although there is evidence of anterior cover feathering on the humerus, the posterior feathering remains unknown (Fig. 1).

Preserved primary remiges and primary coverts project at obtuse angles relative to the longitudinal axis of the wing bones and are recurved medioposteriorly. While extending the distal part of the wing, the primary remiges do not exhibit slotting between the feathers. Secondary feathers and secondary coverts are much shorter and project straight from the ulna. The open forewing of *Microraptor* has a slender V-shaped wingtip formed by the primary feathers (BMNHC PH881, IVPP V13352 and STM 5–9) and has a fan-shaped arm-wing formed by the secondary feathers projecting from the ulna (IVPP V13552) (Fig. 1). The wing shape of *Microraptor* is different from wings of modern birds utilising wind speed gradient soaring (e.g., albatross [48]), those that utilise extensive thermal soaring (e.g., hawks [48] – but see discussion section Microraptor *wing shape and implications on locomotion and foraging behaviour*), burst flapping specialists (e.g., landfowl [49]), and birds utilising wing assisted incline running (WAIR) (e.g., partridges [50]). Instead, *Microraptor* has a wing shape closest to those of living birds flying with continuous or near-continuous flapping gaits at high speeds. Such wings are often simply referred to as "high-speed wings" because of this association [51, 52]. These wings have a lower camber than elliptical wings and, on average, a moderately high aspect-ratio tapering to a relatively compact wingtip that is unslotted or barely slotted (e.g. modern falcons and shorebirds) [51, 52]. However, the forewing of *Microraptor* differs slightly from these wing shapes because of a proportionally larger non-manus portion (arm-wing) compared to the highly slender manus portion (wingtip) (Fig. 1). In contrast, the wings of the iconic early avialans *Anchiornis* and *Archaeopteryx* have been reconstructed with a rounded shape, as seen in some modern passerine birds (elliptical shape) [3, 53] or in some Galliformes (well-rounded wingtip to elliptical shape) [54].

Overall, primary remiges and primary coverts of the forewing of *Microraptor* resemble those of *Archaeopteryx* and *Confuciusornis*, whereas secondary feathers and coverts (except the close-vaned feature), and marginal coverts resemble those of *Anchiornis*. This pattern of primary remiges associated with short primary coverts and secondary feathers associated with long secondary coverts seems to be unique to *Microraptor*. In other microraptorines, the preservation of the forearm feathers is not good enough to describe the pattern of the covert feathers, except in *Zhenyuanlong*, which has both short primary and secondary coverts [55]. The number of each feather type and the number of feather layers seem to be variable in *Microraptor*, especially for covert feathers. However, it seems that in general, *Microraptor* had five layers of feathers in its forewing: one layer of remiges (10 primary remiges and ~17–21 secondary remiges), one layer of greater coverts (10 primary greater coverts and ~17–21 secondary greater coverts), one layer of median coverts (~ 13–16 primary median coverts and ~18–22 secondary median coverts), one layer of lesser coverts, and one layer of marginal coverts. *Microraptor* has been suggested to possess precursors to alula feathers [21]. Under LSF, the morphology of these feathers was better visualised, and they seem to be ventral primary coverts that were folded anteriorly during burial.

Primary remiges

The primary remex count of *Microraptor* is around ten in BMNHC PH881 and STM 5–9. These are asymmetrical close-vaned feathers that curve medioposteriorly, which gives the leading edge of the wing a curved shape, as seen in IVPP V13352 (Fig. 2). By measuring the curvature of the feathers using the rachises and calami, remiges P9 to P7 of *Microraptor* specimen STM 5–9 curve medially between ~10° and ~12° towards the body of the specimen (Fig. 3). In *Confuciusornis* specimen STM 13–45, the same remiges have a slightly smaller curvature than in *Microraptor* (~ 10°). However, *Archaeopteryx* and *Anchiornis* have different primary remex curvatures from *Microraptor*. The *Archaeopteryx* Berlin specimen (HMN 1880) has a remex P9 with less than 5° curvature, whilst remiges P6 to P8 curve laterally away from the body of the animal, instead of medially towards it (Table 1; Table S4 in Additional file 1). On the other hand, *Anchiornis* has feathers that are more curved than those of *Microraptor* and *Confuciusornis*: primary remiges of specimen BMNHC PH828 curve medially between ~15° and ~18° (Table 1; Table S4 in Additional file 1). Differing feather curvatures can also be seen in modern birds: birds of prey like the peregrine falcon (*Falco peregrinus*) and the Eurasian sparrowhawk (*Accipiter nisus*) have primary remiges with medium curvature (between ~8° and ~18°), the domestic chicken (*Gallus gallus*) has primary remiges with high curvature (between ~17° and ~32°), the Californian condor (*Gymnogyps californianus*) has primary remiges which curve laterally instead of medially, and some birds like the sparkling violet-ear (*Colibri coruscans*) have primary remiges that curve laterally in the distal part of the forewing but curve medially in the proximal part of the forewing (Table 1; Table S4 in Additional file 1). The primary remiges of *Microraptor* display trailing vanes with small barb angles as seen in specimens IVPP V13352 and V13320 (~ 20° opening from the rachis), and as previously described in specimen BMNHC PH881 by Feo et al. [56] (18.1°–23.2° opening from the rachis). In comparison, enantiornithines and modern birds have trailing vanes with large barb angles (22.5°–60.0° opening from the rachis) [56]. In the same three *Microraptor* specimens, the leading edges of the primary remiges have small barb angles, giving the leading edge a 'cutting-edge' shape, also seen in *Archaeopteryx*, *Confuciusornis* and modern birds [56]. Cross-linked barbules are not directly observable, but a herringbone pattern with tight straight barbs is visible in the primary remiges of specimen IVPP V13320 and V13352, suggesting the presence of cross-link barbules

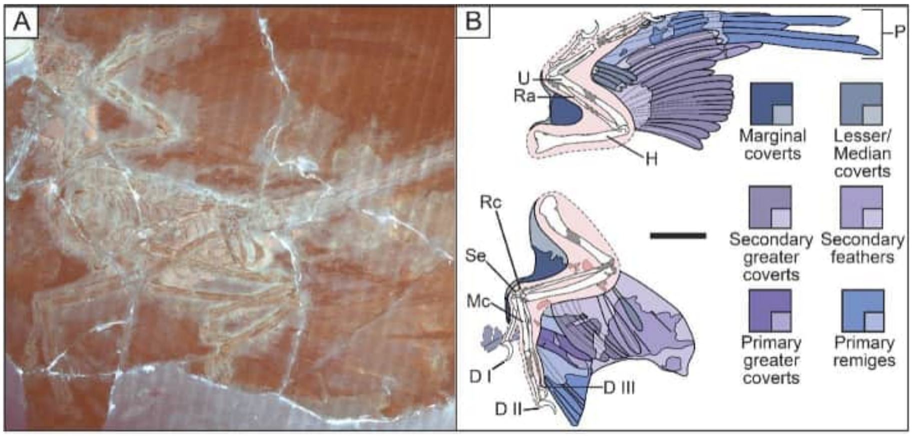

Fig. 2 Forelimbs of *Microraptor* IVPP V13352 showing a well-preserved secondary greater covert series. **A** Under LSF and **B** as an anatomical line drawing. Colour scheme is as follows: darker blues/purples (colours in large boxes), preserved feathers; pale blues/purples (colours in inset boxes), reconstructed feather outlines; white, preserved skeleton; grey, reconstructed skeletal sections; dark pink, preserved soft tissues; pale pink, reconstructed soft tissues. Short-dashed lines are reconstructed outlines. This colour scheme will be used in all figures in this study (Figs. 2, 3, 4, 5, 6, 7, 8, 9, and 10, and S1-4). D, digits with interpreted numbers; H, humerus; Mc, metacarpal; P, primary remiges; Ra, radius; Rc, radiale carpal; Se, semilunate carpal; U, ulna. This specimen preserves the best secondary greater covert series with an estimated count of ~ 17. It also preserves the crescent-shaped semilunate articulating with metacarpals I and II. Scale bar is 50 mm

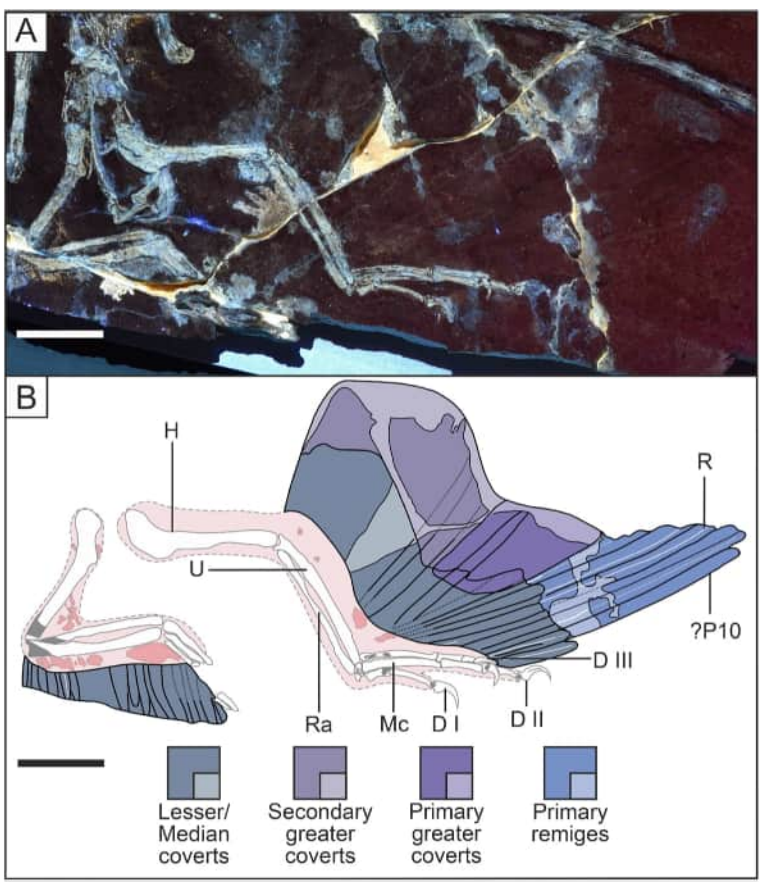

Fig. 3 Forelimbs of *Microraptor* specimen STM 5–9 showcasing longest primary in P9 position. **A** LSF image and **B** as an anatomical line drawing. R, preserved rachis. This specimen has the most extended forelimb position of all the studied specimens, revealing the prominent biceps tuberosity of the radius. It is also the only specimen studied with remex P9 as the longest primary remex. See colour scheme key in Fig. 2. Scale bar is 50 mm

Table 1 Comparison of feather curvature in modern birds and fossil paravians

Species	Mean curvature in °	Max. curvature in °	Min. curvature in °	Direction
Columba livia	10.11	15.7	6.73	medial
Ara ararau	12.9	16.29	9.44	medial
Tichodroma muraria	16.2	19.81	12.59	medial
Falco peregrinus	6.42	10.23	2	medial
Phoebastria immutabilis	5.43	9.32	2.09	medial & lateral
Anas platyrhynchos	5.62	11.96	1.74	medial
Colibri coruscans	9.53	20.32	3.06	medial & lateral
Strix aluco	14.97	19.47	12.27	medial
Accipiter nisus	10.63	18.33	6.71	medial
Gallus gallus	28.53	31.99	23.32	medial
Gymnogyps californianus	7.84	10.64	3.82	lateral
Microraptor sp.	11.52	12.59	10.4	medial
Archaeopteryx sp.	6.27	9.26	1.34	medial & lateral
Anchionis hui	15.25	15.25	15.25	medial
Anchionis hui	17.58	17.58	17.58	medial
Confuciusornis sp.	8.57	18.88	2.09	medial
Confuciusornis sp.	10.94	13.23	9.1	medial

holding the shape of the feathers in *Microraptor*. This feature is also seen in the primary remiges of the microraptorine *Wulong*, and of *Confuciusornis*, as well as modern birds [4, 57]. In contrast, the early bird *Anchiornis* seems to have symmetrical open-vaned primary remiges with no cross-linked barbules [4, 58].

Direction of curvature refers to the bending in direction of the distal end of the wing (lateral curve away from the body of the animal) or the proximal end of the wing (medial curve towards the body of the animal). Detailed measurements are in Table S4 of Additional file 1.

The longest primary remiges of *Microraptor* are substantially longer than the secondary feathers: between 1.4 (STM 5–5; ?P5 compared to ?S3) and 1.7 (IVPP V13352; P5 compared to S3) times longer. The same feature is observed in *Confuciusornis*: the longest primary remex in specimen IVPP V13156 is two times longer than the secondary feathers (260.2 mm compared to 129.2 mm). In contrast, the longest primary remiges of *Archaeopteryx* specimen WDC-CGS-100 and *Anchiornis* specimen BMNHC PH828 are about the same length as the longest secondary feather (WDC-CGS-100: 126.5 mm compared to 125.2 mm; BMNHC PH828: 61.0 mm compared to 63.1 mm). The longest primary remiges are also longer than the primary remiges of the hindwing: 1.1 times longer in STM 5–5 and 5–75 and 1.5 times longer in IVPP V13352 (see Chotard et al. [47]). There does not seem to be a common pattern in the primary remex series. The longest primary of specimen BMNHC PH881 is P3, with P1 and P2 being the shortest primary remiges of the forewing. The most distal feathers of the forewing of specimen BMNHC PH881, P9 and P10, are slightly longer than P1 and P2. This creates a series of primary remiges shaped as a triangle with the proximal edge shorter (P1 to P3) than the distal edge (P3 to P10) (Fig. 4). On the other hand, the longest primary remex of specimen STM 5–9 is P9 with feathers gradually increasing in size distally creating a more uniform posterior wing edge compared to other specimens (Fig. 3). In the incomplete primary remex series of IVPP V13352, small primary remiges are set between the longer ones, creating a dent in the wing profile (Fig. 2). This indentation has been attributed to sequential feather moulting [59].

Secondary feathers

A completely preserved secondary feather series remains unknown, but new feather type records and soft tissues

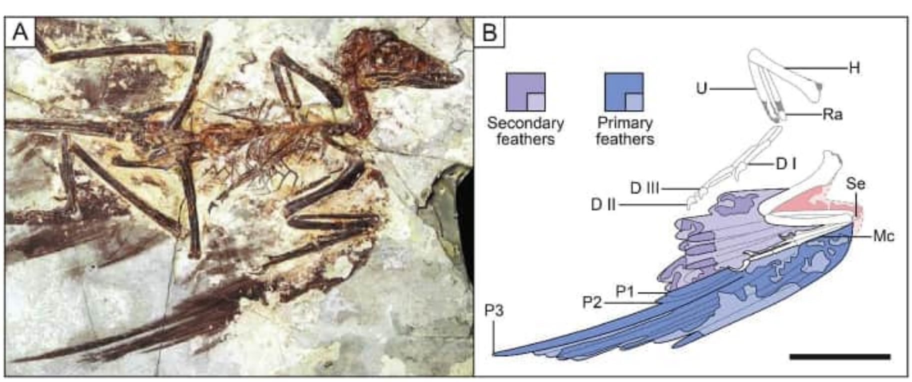

Fig. 4 Forelimbs of *Microraptor* BMNHC PH881 showcasing smallest primaries in P1 and P2 position. **A** Photo of BMNHC PH881 modified from Li et al. [11] and **B** as an anatomical line drawing. See colour scheme key in Fig. 2. Scale bar is 50 mm

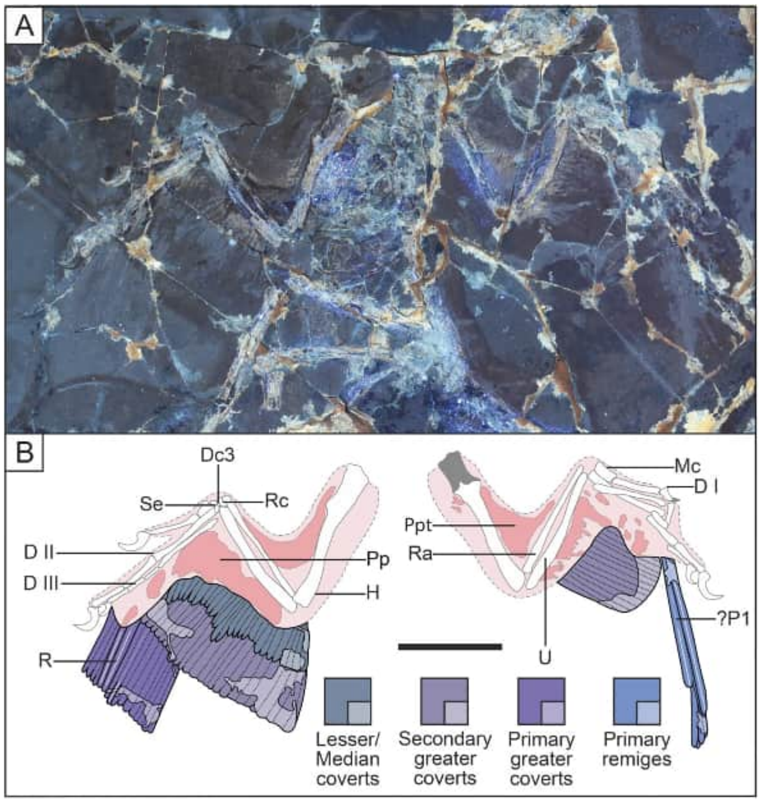

Fig. 5 Forelimbs of *Microraptor* STM 5–93 showcasing the propatagium. **A** LSF image of the slab and **B** as an anatomical line drawing. Dc3, distal carpal 3; Pp, postpatagium; Ppt, propatagium. The specimen preserves the best propatagia and displays feather sheaths of the secondary feathers in the left postpatagium. See colour scheme key in Fig. 2. Scale bar is 50 mm

revealed under LSF help to constrain the inferred secondary feather count. Hidden rachises and feather sheaths highlighted by LSF can be used to infer the number of feathers. The almost complete series of secondary greater coverts of holotype IVPP V13352 has a gap revealing an underlying secondary feather, which suggests a secondary greater covert is missing. Thus, IVPP V13352 must have possessed 17 secondary greater coverts likely associated with 17 secondary feathers (Fig. 2; Table S3 in Additional file 1), close to the original estimate of 18 from Xu et al. [21]. In similar-sized and newly described specimen STM 5–93 (Fig. 5), the secondary feather count could be higher based on the presence and spacing of preserved secondary feather sheaths. The preserved feather sheaths are separated by ~2–3.4 mm across the 56.7 mm long ulnar postpatagium. Based on an average separation of 2.7 mm, this suggests the presence of ~21 secondary greater coverts associated with ~21 secondary feathers. Unlike the primary remiges, the secondary feathers are symmetrically vaned as in *Archaeopteryx* and *Confuciusornis*. However, the secondary feathers are narrower than in *Archaeopteryx* and *Confuciusornis*, resembling the slender feathers of *Anchiornis*, although they are open-vaned in the latter [3, 4, 8] and closed-vaned in *Microraptor*. These feathers project around 90° from the distal end of the ulna and project with acute angles from the proximal end of the ulna. The two preserved distal secondary feathers of specimen IVPP V13352 and the secondary feathers of the proximal portion of the right ulna of specimen STM 5–172 seem to be medioposteriorly curved, as seen in the primary remiges (Fig. 6). In *Anchiornis* specimen BMNHC PH804, secondary feathers of the left forelimb are curved as seen in *Microraptor* specimens IVPP V13352 and STM 5–172. This feature of the secondary feathers can also be found in most modern birds: e.g., common swift (*Apus apus*) (see Fig. 1 from Jukema et al. [60]), Laysan albatross (*Phoebastria immutabilis*) (PSM 10908 [61] and 21,460 [62]), rock pigeon (*Columba livia*) (PSM 11000 [63], 17193 [64], and 20721 [65]).

Primary greater coverts

Series of primary greater coverts are partially preserved across different specimens. Based on the width of the primary greater coverts preserved in specimens IVPP V13352 (~ 10 mm) and STM 5–221 (~ 3 mm), and the

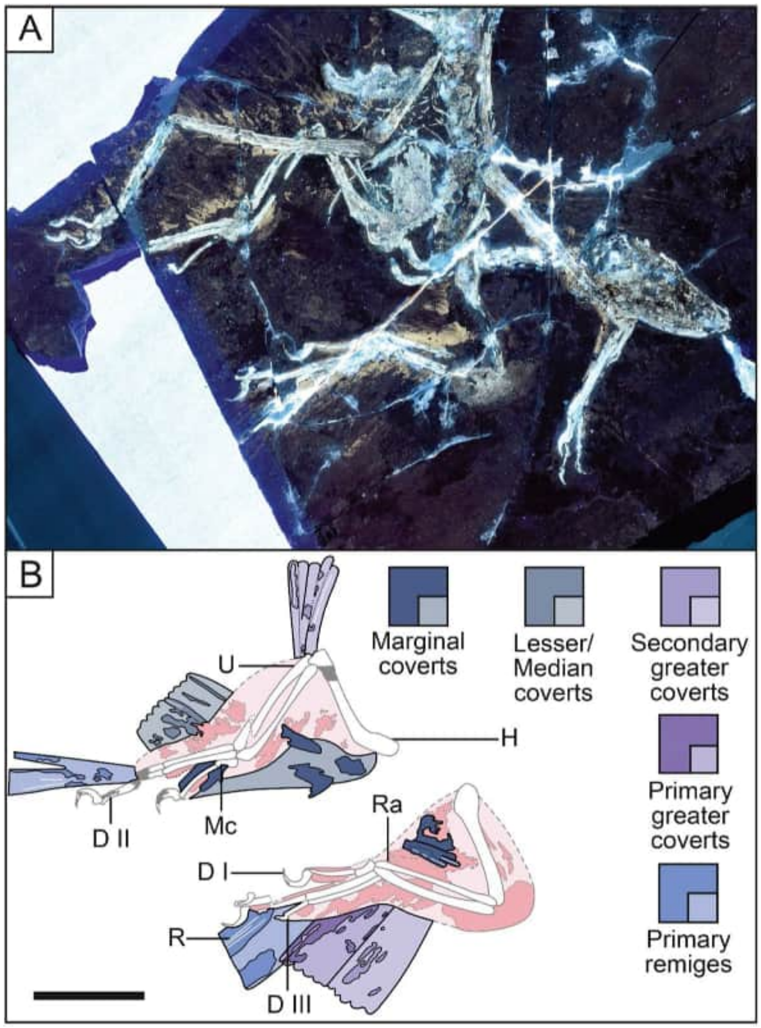

Fig. 6 Forelimbs of *Microraptor* STM 5–172 with marginal coverts in life position in the propatagium. **A** LSF image of the counterslab and **B** anatomical line drawing. The specimen displays the original arrangement of the marginal coverts. Instead of lying anterior to the forelimb, the marginal coverts are preserved in anatomical position: projecting perpendicular to the wing profile in the propatagium, as seen in modern birds. See colour scheme key in Fig. 2. Scale bar is 50 mm

number of primary remiges in specimens BMNHC PH881 and STM 5–9 (Table S3 in Additional file 1), we infer ten primary greater coverts in *Microraptor*. It is not possible to observe the degree of vane asymmetry or whether the feather was open or closed-vaned, but these could be asymmetrically closed-vaned feathers based on the hindwing [47]. It is also hard to tell if the primary greater coverts project from the metacarpals and digits with the same angles as the primary remiges, as no *Microraptor* specimen has a fully preserved primary greater covert overlapping the associated primary remex. However, in specimen STM 5–4, the primary greater coverts of the right forewing project from the soft tissues of the manus with an angle of ~157°, while the primary remiges of the left forewing project with an angle of ~161° (Fig. 7). The primary greater coverts preserved in the right forewing of the specimen are located more proximally than the primary remiges preserved in the left forewing, which could explain the slight difference in angle, with feathers of the wing becoming more angled distally. The primary greater coverts seem curved like the primary remiges in specimens IVPP V13352 and STM 5–75 (Figs. 2 and 8), but in specimen STM 5–221 they are straight (Fig. 9).

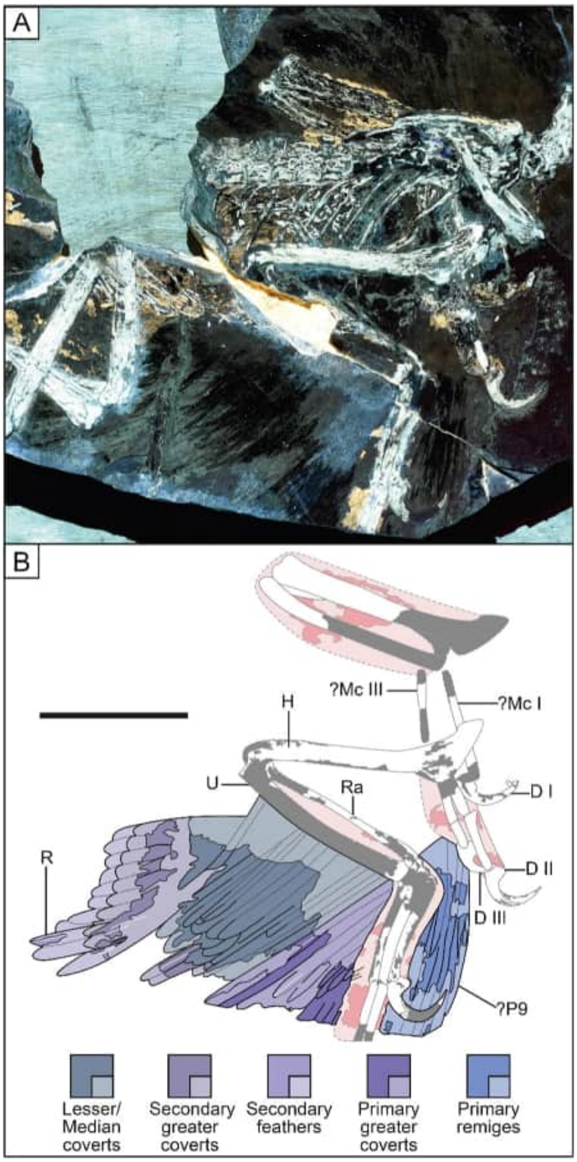

Fig. 7 Forelimbs of *Microraptor* STM 5–4 showcasing the lesser and median coverts. **A** Under LSF and **B** as an anatomical line drawing. This specimen is the only one with distinguishable layers of lesser and median coverts, indicating that *Microraptor* potentially possessed five layers of feathers on its forewing. See colour scheme key in Fig. 2. Scale bar is 50 mm

Secondary greater coverts

Secondary greater coverts have symmetrical vanes and are closed-vaned, perfectly overlapping the associated secondary feathers as seen with the preserved rachises in the right forewing of specimen IVPP V13352 (Fig. 2). This feature is also seen in *Anchiornis, Archaeopteryx, Confuciusornis*, and modern birds [3, 8]. *Microraptor* also shares the feature: long secondary greater coverts; with *Anchiornis* and *Archaeopteryx*, despite having proportionally shorter primary greater coverts than both of these early paravians. The shortened primary greater coverts resemble those of *Confuciusornis* (IVPP V13156: 115.8 mm compared to 260.2 mm) and modern birds. In IVPP V13352, we can estimate the number of secondary greater coverts to be 17 (see Secondary Feathers section above) and their length to be ~0.76 times the length of secondary feathers. It is also the only specimen with observable posteriorly curved secondary greater coverts, with these feathers being seemingly straighter in other specimens like STM 5–93 and 5–4 (Figs. 5 and 7). Specimen STM 5–93 also seems to have more secondary greater coverts (~ 21) than similar-sized specimen IVPP V13352 (see Secondary feathers section above).

Median and lesser coverts

No complete set of median primary or secondary coverts is observable in the studied specimens, despite specimen STM 5–9 preserving faint outlines of the median coverts from the proximal end of the ulna to the distal end of the palm of the left arm (Fig. 3). In addition, specimen STM 5–93 has faint outlines of median coverts from the middle of the manus to the end of the ulna (Fig. 5), and specimen STM 5–109 has median covert imprints spread across the right forelimb (Fig. 10). Specimen STM 5–109 has ~19 median primary coverts along the manus and ~30 median secondary coverts along the ulna based on preserved feather tips and feather width, which makes STM 5–109, the specimen with the most median coverts at ~49 (Fig. 10; Table S3 in Additional file 1). Other specimens with distinguishable median covert widths have an estimated count of ~35: between 13 (STM 5–93) and 16 (STM 5–221) median primary coverts, and between 18 (IVPP V13352) and 22 (STM 5–93) median secondary coverts (Figs. 2, 3, 5, 7, 9, and 10; Table S3 in Additional file 1; Fig. S1 in Additional file 2). Specimens STM 5–4 and 5–221 seem to indicate that *Microraptor* could have at least three layers of primary and secondary coverts: one layer of greater coverts, one of median coverts, and one of lesser coverts (Fig. 1). As the preservation in specimen STM 5–109 is poor, with the right arm folded and feathers that are clumped proximodistally, two layers of additional coverts could explain why the count in this specimen is so different from IVPP V13352 as well as STM 5–93 and 5–221. The correct count in specimen STM 5–109 could be ~35 of median primary and secondary coverts with ~15 feathers mixed from the layer of lesser coverts.

Median coverts and lesser coverts from the manus and ulna are symmetrically closed-vaned and straight. They also seem to project from the bones with similar angles to primary greater coverts along the manus, and to secondary greater coverts along the forearm. Additional layers

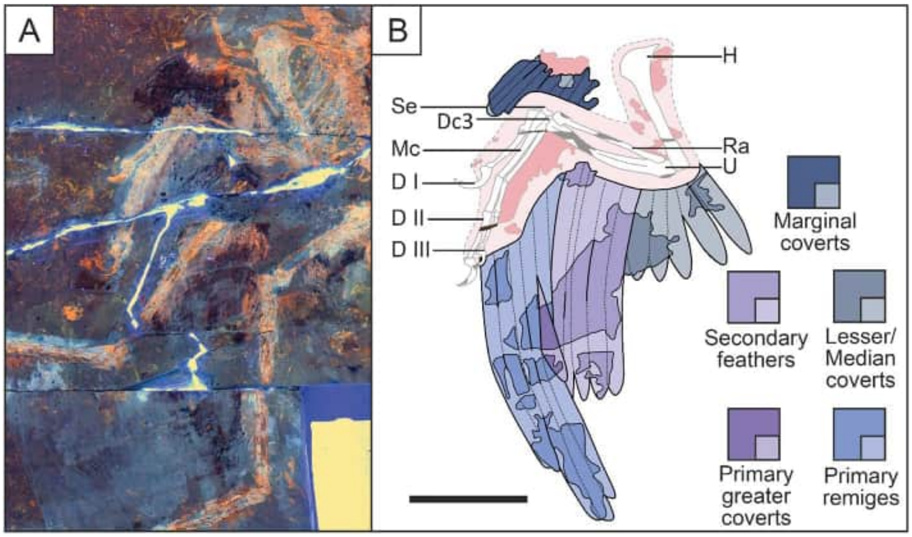

Fig. 8 Forelimbs of *Microraptor* STM 5–75 showcasing distal carpal 3. **A** LSF image of the slab and **B** as an anatomical line drawing. This is the only studied specimen preserving a distal carpal 3 in anatomical position, completing the wrist of *Microraptor* (semilunate + radiale) with a third bone. See colour scheme key in Fig. 2. Scale bar is 50 mm

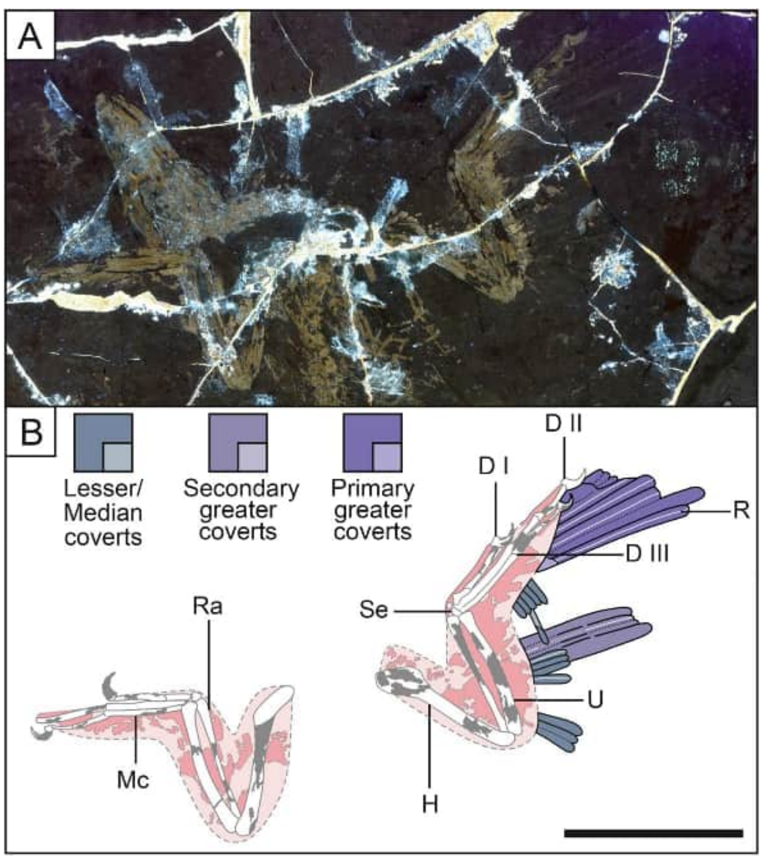

Fig. 9 Forelimbs of *Microraptor* STM 5–221 showcasing the soft tissues preserved alongside the bones. **A** Under LSF and **B** as an anatomical line drawing. The specimen preserves extensive soft tissues, including those of the shoulder. See colour scheme key in Fig. 2. Scale bar is 50 mm

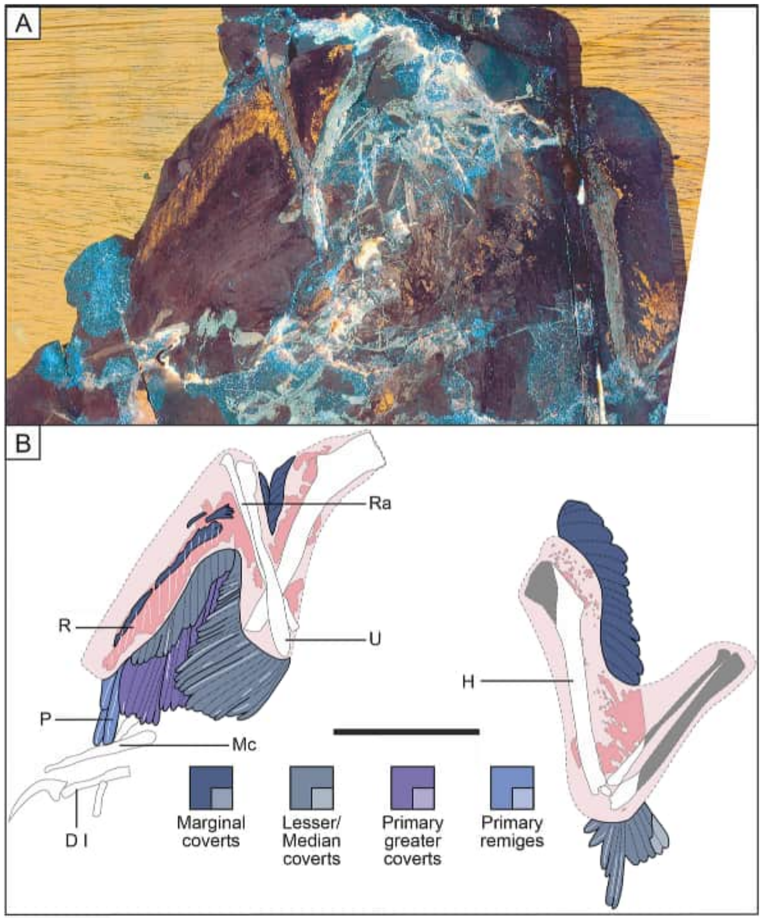

Fig. 10 Forelimbs of *Microraptor* STM 5–109 showcasing upper arm feathering and the postpatagium. **A** LSF image of the counterslab and **B** as an anatomical line drawing. The specimen preserves the only feathers found from the upper arm of *Microraptor*. It also displays an exceptionally preserved postpatagium (manus section) with the feather sheaths of the primary remiges and primary greater coverts. See colour scheme key in Fig. 2. Scale bar is 50 mm

of coverts are also found in other early paravians. In the reconstruction of the wing of *Anchiornis* from Longrich et al. [3] there are four layers of primary coverts (one layer of primary greater coverts, one of median primary covert, and two of lesser primary coverts) and three to four layers of secondary coverts (one layer of secondary greater coverts, one of median secondary feathers, and one or two of lesser secondary feathers). In *Archaeopteryx*, long primary greater coverts have been described from rachises imprints on the counterslab of specimen HMN 1880 by Longrich et al. [3]. Considering this information, there seems to be at least one additional layer of primary coverts in *Archaeopteryx* based on the slab of HMN 1880: the layer of median primary coverts. Secondary coverts of *Archaeopteryx* are only observable in specimen HMN 1880, and only a single layer of secondary greater coverts seems preserved. For *Confuciusornis*, the covert pattern is not clear, but it seems to possess two layers of minor primary coverts and four layers of minor secondary coverts [3, 66]. Modern birds also have variable numbers of covert layers depending on the species. The common swift (*Apus apus*) has three layers of coverts: primary/secondary greater, median, and lesser coverts (see Fig. 1 from Jukema et al. [60]); while the Laysan albatross (*Phoebastria immutabilis*) has three layers of primary coverts (greater, median, and lesser coverts) and four layers of secondary coverts (greater, median and two layers of lesser secondary coverts: PSM 10908 [61] and 21460 [62]). The rock pigeon (*Columba livia*) possesses only two layers of primary coverts (greater and median) with at least six layers of secondary coverts (greater, median, and at least four layers of secondary lesser coverts: PSM 11000 [63], 17193 [64], and 20721 [65]).

Marginal coverts

Marginal coverts in *Microraptor* are reported here for the first time. They are also the only feathers to have been observed along the humerus, and the only feathers to be preserved on the opposite side of the wing. No complete set has been observed in any single specimen, but they are preserved across specimens from the top of the humerus to the middle of digit II. They are often preserved as amorphous patches of integument, but in specimen STM 5–109, they can be identified as straight and symmetrically closed-vaned feathers (Fig. 10). Combining observations from the different specimens studied, *Microraptor* had a similar marginal covert pattern as *Anchiornis*. In *Anchiornis* specimen STM 0–144, feathers become shorter and more angled distally along the wing, between ~130° and ~140° to the radius and manus. In specimen STM 5–109, marginal coverts of the humerus are angled ~60° on the proximal part of the deltopectoral crest, then ~100° on the distal part of the deltopectoral crest, and finally ~140° on the distal end of the humerus (Fig. 10). In specimen STM 5–172, marginal coverts are preserved in the propatagium and along the manus (Fig. 6). The feathers in the propatagium are angled between ~40° and ~60° from the distal portion of the humerus and ~150° from the proximal portion of the radius, so the feathers are angled between ~40° and ~150° to the leading edge. In modern birds, marginal coverts are angled perpendicular to the wing plane anteriorly and successive layers of different coverts transit to a parallel alignment with the wing plane posteriorly [67]. Thus, the preserved perpendicular marginal coverts in the propatagium of specimen STM 5–172 are suggesting that *Microraptor* had leading edge feathers organised in the same pattern as modern birds.

Alula feathers

Xu et al. [21] mention the presence of feathers associated with the short manual digit I (numbered digit II in Xu et al. [21]) of *Microraptor* IVPP V13352 and the possibility that these feathers are precursors to the alula. These feathers appear in the same anatomical position as the alula feathers present in the enantiornithine *Eoalulavis* and in later diverging birds including Neornithes [68]. However, under different lighting conditions and under LSF, these feathers in IVPP V13352 seem to continue under digit I, all the way to digit II (Fig. 2). This suggests that they are ventral primary coverts that were folded anteriorly when the animal died. In addition, no other *Microraptor* specimen studied has preserved these feathers, despite their similarly exceptional preservation. Feathers are associated with manual digit I in the anchiornithid *Caihong juji* (specimen PMoL-B00175), but further work is needed to evaluate whether they are alula feathers [68]. However, alula feathers are absent in some early paravians such as *Archaeopteryx* and *Confuciusornis*.

Skeleton

The forelimb skeleton of *Microraptor* has been described in several past studies, including Xu et al. [22], Hwang et al. [69], Xu et al. [21], Gong et al. [19], Turner et al. [20], and Pei et al. [10]. In this study, we make use of a larger sample adding ten new and different-sized specimens to extend our knowledge of the forelimb skeleton. The forelimb lengths of the different specimens are estimated (humerus + ulna + metacarpal II + digit II) between 154 mm (BMNHC PH881) and 272 mm (STM 5–142) with estimated body masses between 0.22 kg (BMNHC PH881) and 2.13 kg (STM 5–142). Specimens STM 5–9, 5–93, 5–150, 5–172 and 5–221 have large deltopectoral crests extending over one third the length of the humerus. Other specimens have shorter deltopectoral crests expanding over less than one third the length of the humerus, as seen in other microraptorines from the figures of Poust et al. [57], Xu and Qin [70], Zheng et al. [71]. However, studied *Microraptor* specimens with 'short' deltopectoral crests still have proportionally larger deltopectoral crests than those of *Anchiornis* [72]. *Confuciusornis* specimens have deltopectoral crests extending over one third the length of the humerus [73, 74] and share this feature with studied *Microraptor* specimens with 'large' deltopectoral crests, and with *Archaeopteryx* specimens HNM 1880 and WDC-CGS-100. The quadrangle shape of the deltopectoral crest of *Microraptor* resembles that of *Archaeopteryx*, but it differs greatly from the semi-circle shaped one of *Confuciusornis*. Manual phalanges I are short with Mc I+ Phx I-1:Mc II length ratios between 0.8 (STM 5–142) and 0.94 (STM 5–75). These ratios are smaller than those of *Archaeopteryx* and *Confuciusornis* (ratios higher than 1) and closer to those seen in most modern birds (0.3 to 0.69; Table S3 in Additional file 1) including Columbiformes, Anseriformes, Charadriiformes, Passeriformes, Piciformes and Sphenisciformes. There does not seem to be a correlation between the size of preserved individuals and the difference in deltopectoral expansion or the length of digit I. Combining observations from different specimens allowed the full wrist to be described. It is composed of a radiale, a semilunate carpal, and a distal carpal behind digit III, a wrist configuration intermediate between those seen in dromaeosaurids like *Deinonychus* and early birds like *Sapeornis* [75, 76]. In some specimens, LSF reveals preserved keratinous claw sheaths that have only been described previously in specimen LVH 0026 [19].

Pectoral girdle

The pectoral girdle of *Microraptor* is well-represented by preserved scapula, coracoid and furcula bones [10, 19, 21, 69]. The scapulae are best preserved in specimens STM 5–9, 5–75 and 5–142 as well as IVPP V13352 (scapulae of STM 5–4 and 5–150 are fragmentary, especially in the latter). The scapulae shafts of *Microraptor* are longer compared to those of *Anchiornis*, *Archaeopteryx* and *Confuciusornis*, but still shorter than the length of the humerus as previously reported by Pei et al. [10]. Overall, the scapulae are strap-like and slightly curved dorsally in STM 5–4, 5–9, 5–75 and 5–142 as well as IVPP V13352. The acromion process of the scapula was only visible in STM 5–4, 5–9 and 5–75 but is not as prominent as in *Microraptor* CAGS 20–8-001 (see Hwang et al. [69]), which may be potentially linked to fossil taphonomy.

Coracoids are preserved in lateral view in *Microraptor* IVPP V13352 and STM 5–75, and in lateroanterior view in specimen STM 5–9 revealing a large coracoid fenestra, as seen in specimen LVH 0026 [19] and in the microraptorine *Wulong* [57]. However, unlike in *Wulong*, no coracoid foramen was visible in *Microraptor* specimens of this study (IVPP V13352 and STM 5–9 and 5–75). In the absence of preservation of the coracoid in dorsal view, the exact shape of this bone in *Microraptor* could not be determined. In specimens STM 5–9 and 5–75 as well as IVPP V13352, scapulae and coracoids are tightly articulated and fused together at an angle between 90° and 105°, positioned parallel to the axial skeleton, as seen in *Microraptor* specimens LVH 0026 and CAGS 20–8-001 [19, 69]. The scapulocoracoids of *Microraptor* form a L-shape in lateral view similar to those of troodontids [77] and extant flightless birds like ostriches (see Wu et al. [77] and Kassem et al. [78]). However, unlike troodontids and extant flightless birds, the coracoids of *Microraptor* have an important flexure similar to those of *Archaeopteryx* and *Buiteraptor* [79]. The scapulocoracoid articular surface is visible in IVPP V13352 and STM 5–75 with a laterally facing glenoid fossa. This condition is the same as in other dromaeosaurids including microraptorines *Sinornithosaurus* and *Changyuraptor*, unenlagiines, and *Bambiraptor* [77]. There have been many morphological changes to the articulation of the scapulocoracoid in paravians [77] and the timing in ontogenetic transformation of the articulation seems to have changed as well [80]. The scapula and coracoid of *Wulong* are unfused in the only known juvenile specimen DNHM D2933 [57], which suggests that a fused scapulocoracoid is a feature of adult microraptorines. However, they are known to fuse before skeletal maturity in *Confuciusornis* [80], whereas, in *Anchiornis* and *Archaeopteryx* they are unfused in known mature specimens [72, 81]. *Microraptor* specimens STM 5–9 and IVPP V13352 are larger than STM 5–75, but are not the largest, suggesting that it could be possible that the fusion of the scapulocoracoid happens before skeletal maturity, as in *Confuciusornis*.

Although disarticulated from the rest of the pectoral girdle, the furculae are preserved in *Microraptor* STM 5–75, 5–142 and 5–221. They are well-preserved boomerang-shaped with a dorsoventrally flattened cross section and lacking a hypocleidum, similar to those of specimens CAGS 20–8-001 [69] and LVH 0026 [19]. The furcula is similar to those of other dromaeosaurids (e.g., *Bambiraptor*, *Buitreraptor* and *Velociraptor*) [82] and anchiornithine birds (see Wu et al. [77]). In contrast, other early avialans including *Archaeopteryx* and *Confuciusornis* have thicker, U-shaped furculae (see Wu et al. [77] and Nesbitt et al. [82]).

Humerus

The humeral shaft is only slightly thicker than the ulna shaft, as seen in *Microraptor* specimen CAGS 20–8-001 [69]. It is bowed anteriorly, as seen in other maniraptorans [83]. *Microraptor* displays a prominent humeral head supported by the internal tuberosity and the deltopectoral crest. The well-developed internal tuberosities are preserved in specimens STM 5–9, 5–4 and 5–221 (Figs. 5, 7 and 9). The deltopectoral crest has a low-width rectangular form with a wider distal end than the proximal end, as seen in *Archaeopteryx* [84, 85]. In contrast, *Confuciusornis* has a wide semi-circular shaped deltopectoral crest. The same shape can be seen in the left arm of *Microraptor* specimen STM 5–150, but this may be a preservation artifact, as the deltopectoral crest of the other arm does not have the same shape and the bones are fragmented (Fig. S2 in Additional file 2). The deltopectoral crest was measured in 11 specimens, six of them (BMNHC PH881, IVPP V13352 as well as STM 5–5, 5–75, 5–109, and 5–142) have deltopectoral crests expanding less than one third of the length of the humerus, whilst the five remaining specimens (STM 5–9, 5–93, 5–150, 5–172, and 5–221) have deltopectoral crests expanding over one third of the length of the humerus. Deltopectoral crest expansion seems to be independent from the size of the individual as specimen STM 5–150 has a longer deltopectoral crest than similar-sized specimen STM 5–5. A small, distinctive ovoid foramen is present in the thinnest portion of the deltopectoral crest of the right humerus of specimen BMNHC PH881 as described by Pei et al. [10]. This feature has also been observed in specimens STM 5–5, 5–9 and 5–150 (crushed in this specimen), but could not be confirmed in other specimens due to insufficient preservation (Fig. 3; Figs. S1 and S2 in Additional file 2). It is also present in the deltopectoral crests of *Confuciusornis*, but absent in early paravians such as *Anchiornis* and *Archaeopteryx* [72–74, 85].

Ulna

The ulna is bowed posteriorly as seen in other maniraptorans [83]. In specimens that preserve both ends of the ulna (IVPP V13320 and V13352; STM 5–5, 5–9, 5–75, 5–142, 5–150, 5–172 and 5–221), the proximal end is quadrangular and the distal end is rounded. The ulna is roughly the same size or slightly shorter (~ 1 cm less) than the humerus. The ulna midshaft also has the same thickness as the humerus midshaft.

Radius

The radius is straight and slightly shorter than the ulna. The radius is also shorter than the humerus, between ~ 0.7 and ~ 0.9 the length of the humerus, except for specimens STM 5–9 and 5–75 which have a radius roughly the same length as the humerus (Figs. 3 and 8). Comparing with the measurements from Benson and Choiniere [86] and Middleton and Gatesy [87], the two specimens of *Microraptor* have similar radius:humerus proportions as avialans and modern birds. However, it should be noted that neornithines have a large range of radius:humerus proportions. Overall, *Microraptor* seems to have a mean radius:humerus ratio slightly greater that those of other dromaeosaurids.

At midshaft, the radius is ~ 0.6 times as thick as the ulna in specimens BMNHC PH881, IVPP V13320 and V13352 as well as STM 5–9, 5–75, 5–142, 5–172 and 5–221. In contrast, the radii of specimens STM 5–4, 5–5 and 5–93 are much thinner than the ulnae at mid-shaft (~ 0.3 to 0.5 times as thick). Specimen STM 5–150 displays two different conditions: the right radius is ~ 0.6 times as thick as the right ulna, whereas the left radius is only slightly thinner than the left ulna (as seen in IVPP V12230). However, STM 5–150 bones are fragmented and the left ulna is partially hidden by the left humerus, so it is most likely that the left radius thickness would also fall in the ~ 0.6 ratio. Thus, the majority of specimens have radii mid-shafts ~ 0.6 times the width of the ulnae mid-shafts (n = 11). This ratio falls within the range of many other non-avialan dinosaurs, *Confuciusornis* and modern birds [73, 88].

Xu et al. [21] described a prominent biceps tuberosity on the proximal end of the radius in IVPP V13352 (Fig. 2). It has also been observed in STM 5–9 and 5–142 (Fig. 3; Fig. S3 in Additional file 2). In STM 5–142 and IVPP V13352, the humerus, radius and ulna are displaced, helping to make this feature visible. In specimen STM 5–9, the prominent biceps tuberosity on its left radius can be observed with the humerus-ulna-radius articulation in place but with a greatly extended arm. The same tuberosity has been observed in other microraptorines, but it is not as prominent as in *Microraptor* [70, 89]. This feature has not been observed in *Anchiornis* and *Confuciusornis* [72, 73] and is absent in *Archaeopteryx* [84].

Carpals

Radiales are preserved in specimen IVPP V13320 as well as STM 5–5, 5–142 and 5–221, but appear to be the best preserved in specimens IVPP V13352 and STM 5–75 (Figs. 2 and 8). The radiales of these specimens have a subtriangular shape and a concave proximal facet that articulates with the distal end of the radius. *Microraptor* seems to have proportionally large radiales, as large as the semilunate, as seen in *Anchiornis*, *Confuciusornis* and in modern birds [72, 73, 90].

Semilunates are preserved in specimens IVPP V13352 and V13320, BMNHC PH881 as well as STM 5–75, 5–93, 5–142, 5–150 and 5–221 and appear to be better preserved compared to the radiales. Semilunates capping metacarpals (Mc) I and II are crescent-shaped in most specimens. However, for some specimens, the differences in position and/or shape are associated with taphonomy. In specimen STM 5–75 and 5–93, the manus and carpals are displaced posteriorly and anteriorly, respectively. In the highly fragmentary specimen STM 5–150, the semilunate only caps Mc II in the left manus, but a partial bone near the semilunate of the right manus indicates it is broken and would also cap Mc I (Fig. S2 in Additional file 2). In specimen STM 5–221, the semilunate caps Mc II and III in the right manus, but the semilunate and the proximal portions of Mc II and III are broken. The broken piece of the semilunate, located anteriorly to the rest of the bone and distally to Mc I, indicates that the semilunate must have capped Mc I (Fig. 9). The semilunates from specimens IVPP V13320 and V13352 cover the whole proximal end of Mc I and II, whereas in the previously described specimen CAGS 20–7-004, the semilunate covers only half of Mc I and II [55, 69]. Based on new observations, the semilunate of *Microraptor* is found to be similar to the condition in *Changyuraptor*, *Anchiornis* and *Archaeopteryx*, articulating with both Mc I and Mc II (see [72, 84, 91]). This differs from those of *Graciliraptor* and *Confuciusornis*. In *Graciliraptor*, it only contacts metacarpal II [89]. In *Confuciusornis*, the semilunate is fused to the Mc II and III complex, as in modern birds [73].

The final bone of the wrist, distal carpal 3, has only been observed in two specimens, STM 5–93 and 5–75 (Figs. 5 and 8). These small wrist bones tend to be harder to preserve [75, 92]. The distal carpal 3 has a quadrangular shape and is about one quarter the width of the radiale of the respective specimens. Although both specimens have taphonomic displacement in the wrist, the distal carpal 3 of STM 5–75 is in place. Thus, it would be positioned between the ulna and the semilunate in life. The wrist bones of *Microraptor* resemble those seen in *Deinonychus* and several other non-avian maniraptorans [69, 75, 76, 93].

Metacarpals

Metacarpals (Mc) II and III are subequal to equal in length. Mc II is broader than Mc III in all specimens studied, except for specimens IVPP V13352 and STM 5–150, where they have a Mc II that noticeably narrows at the midshaft (Fig. 2; Fig. S2 in Additional file 2). This combination of a broad Mc II as well as Mc II and Mc III of subequal to equal length can also be seen in *Anchiornis* and *Archaeopteryx* [72, 84]. *Confuciusornis* also has a broader Mc II than Mc III, but Mc II does not narrow down at the midshaft [73]. Mc I is short in every *Microraptor* specimen studied: length ratios of Mc I + phalanx I-1 vs. Mc II are estimated between 0.8 (STM 5–142) and 0.96 (STM 5–172). This condition is also found in some other microraptorines. Ratios between 0.68 and 0.72 are observed in *Wulong* [57], ~ 0.94 in *Graciliraptor*, and 0.80 in *Changyuraptor* [91]. However, this is not the case for *Zhenyuanlong* which has a ratio of 1.09 [55] as well as the potential microraptorine *Tianyuraptor* with a ratio of 1.07. These latter two taxa show a similar condition to *Archaeopteryx* and *Confuciusornis*, which also share ratio values greater than 1.

Phalanges

In most specimens that preserve a complete manus (BMNHC PH881, IVPP V13352 as well as STM 5–9, 5–75, and 5–93), digit I has two phalanges, digit II has three phalanges, and digit III has four phalanges. However, specimens STM 5–221 and IVPP V13320 only have three phalanges in digit III (Fig. 9; Fig. S4 in Additional file 2). In every specimen studied, digit II is the longest digit of the manus and possesses the broadest phalanges, except in specimen STM 5–9 where phalanges II-1 and III-1 are equally broad (Fig. 3). Specimens IVPP V12230 and STM 5–109 do not preserve the manus. With digits II measuring between 41 mm (STM 5–221) and 70 mm (STM 5–9), *Microraptor* has an elongated manus like other deinonychosaurians [94] and the same can be observed in *Anchiornis* and *Archaeopteryx* [72, 84, 90]. Specimens IVPP V13352, BMNHC PH881 as well as STM 5–5, 5–9, 5–75, and 5–93 have an extremely short phalanx III-2 and a thin and bowed phalanx III-3 (Figs. 2, 3, 4, 5 and 8; Fig. S1 in Additional file 2) as seen in other dromaeosaurids, including some other microraptorines (e.g., *Graciliraptor*) [89, 94]. Although specimens IVPP V13320 and STM 5–221 have one less phalanx in digit III compared to other *Microraptor* specimens, they also have a thin and bowed phalanx before the ungual. There are nine specimens that preserve partial or complete keratinous sheaths at the tip of their manual unguals: BMNHC PH881, IVPP V13320 and V13352 as well as STM 5–4, 5–75, 5–93, 5–150, 5–172 and 5–221. Specimens IVPP V13352 and STM 5–150 do not preserve the keratinous sheath of ungual III, and STM 5–172 does not preserve the keratinous sheath of ungual II. The manual claws are more recurved than the pedal claws in *Microraptor* (see Chotard et al. [47]). The keratinous sheaths increase the length of the unguals and give them a strongly recurved shape, increasing the curvature from ~ 110° to ~ 160°. In most specimens, ungual III is less recurved than ungual II as seen in specimen LVH 0026 (19). However, overall, the claw of digit III is more recurved (~ 160°) than the claw of digit II (~ 155°), which is more recurved than the claw of digit I (~ 150°) (Table S5 in Additional file 1). The differences in claw curvature are minimal in manual unguals.

Soft tissues

LSF revealed the outline and surface texture of the forelimb of *Anchiornis* [34, 95]. Similar details were uncovered in *Microraptor,* including the shape of the propatagium and postpatagium (Figs. 5 and 10). These soft tissues fluoresced pink. LSF also revealed feather sheaths in several specimens. Preserved soft tissues suggest that *Microraptor* had a strong arm, starting with a relatively large deltopectoral crest and associated soft tissue profile as seen in the humerus of specimen STM 5–221 [12]. Similar to *Anchiornis* [34] and modern birds, the soft tissues forming the propatagium cover more surface area between the humerus and radius than the soft tissues forming the postpatagium between the ulna and the manus. Combining the preserved propatagia in the forelimbs of specimens STM 5–93 and 5–172, we can deduce that the propatagium of *Microraptor* extended from the shoulder to the wrist, with a larger amount of soft tissues along the humerus and a profile slimming down along the radius. This propatagium profile is also seen in modern birds [96] and in *Confuciusornis* specimens STM 13–54 and 13–55 [12]. The posterior side of the forearm slims down smoothly after reaching the phalanges, with the postpatagium expanding all the way to the penultimate phalanx of digit II. The soft tissues of digits II and III appear combined while digit I is separate. This suggests that digit III is almost totally embedded in the postpatagium with only the ungual peeking out, as seen in specimen STM 5–221 (Fig. 9). In modern birds, the same digit is completely embedded in the postpatagium [97]. On the palmar side of digits I and II, *Microraptor* possesses thin and flat phalangeal soft tissues, especially well displayed in the right manus of specimen STM 5–221. Specimens STM 5–4 and 5–172 also display the same soft tissues of the manus as specimen STM 5–221 (Figs. 6 and 7). However, the manus scales are only present in specimen STM 5–221. They are composed of small subcircular reticulate scales (~ 0.5 mm to 0.8 mm across) and are tightly appressed to one another (Fig. S5A in Additional file 2). The reticulate manus scales of *Anchiornis* specimen STM 0–7 [34, 95], are similar to those of *Microraptor*. The manual scales of *Microraptor* differ from its pes scales in lacking distinct pads [33]. Although the soft tissues of digits II and III appear combined, the palmar surface of digit III in specimen STM 5–221 has the same small reticulate scales as the other digits. In specimens STM 5–172, 5–221, and 5–109, the preserved calami of the primary and secondary feathers are embedded deeply in the soft tissues of the postpatagium (Figs. 6, 9 and 10), as in modern birds [8, 97].

Discussion

Microraptor wing shape and implications on locomotion and foraging behaviour

Microraptor has been one of the most intensely studied fossil paravians in terms of documenting early paravian flight potential and evolution, yet there is still much about it that is unknown. Even the four key and widely studied specimens (IVPP V12330, V13352, and V13320 as well as BMNHC PH881), while preserving many features in exquisite detail, do not preserve all the details of the forewing anatomy. Thus, new specimens preserving different features of the forewing anatomy (even if the overall preservation might look less interesting than the key specimens in the literature) provide invaluable information to refine our understanding of the animal.

The newly described specimen STM 5–9 shows the most extended wing (elbow angle ~118°) and is the only studied specimen with the longest primary remex in position P9. In contrast, *Microraptor* specimens with more folded wings have the longest primary remex located more proximally than in specimen STM 5–9 (e.g., position P4 or P3 position in BMNHC PH881 and IVPP V13352 respectively). In some modern birds, such as passerines and the golden eagle (*Aquila chrysaetos*), "proximal primaries" grow faster than "wing-tip primaries" during ontogeny [98]. This suggests that the different length pattern in primary remiges of the bigger *Microraptor* STM 5–9 individual (1.7 kg) compared to the smaller BMNHC PH881 (0.2 kg) and IVPP V13352 (0.9 kg) individuals could be the result of differences in their ontogenetic stages. The primary remiges of *Microraptor* from the inner-edge of the manus would grow faster than the primary remiges of the outer-edge, as seen in some modern birds. Nevertheless, even with this difference in primary remex lengths, they seem to form a V-shaped wingtip in all *Microraptor* specimens. Among modern birds, compact, unslotted and V-shaped wings are most often observed in species specialised to sustained high speeds [99]. These modern birds tend to have a low drag profile, prolonged flight capabilities, and high cruising speeds as typified by a wide range of shorebirds, waterbirds, and falcons [51, 100]. Of the modern birds with such wing shapes, many falcons are high-agility aerial pursuit predators [101, 102]. This is of particular interest as some evidence supports aerial hunting in *Microraptor*, including bony and soft tissue foot anatomy [33] and preserved meals showing predation on birds [103]. In addition, *Microraptor* consumed other small vertebrates (e.g., mammals, lizards, and fishes) [24, 104, 105] similar to the diverse diet adopted by many falcons [106, 107].

It should be emphasised that these lines of evidence help us to infer about the flight dynamics of *Microraptor*, not the kinematics of its flight, and do not indicate that the overall flight performance of *Microraptor* would match that of living falcons. For a start, falcons possess much larger flight muscle fractions than *Microraptor*. The smallest flight muscles among falcons are reported in Eurasian kestrels (*Falco tinnunculus*) with flight muscle fractions as low as 12.2% [108, 109]. These values are still substantially greater than those estimated for *Microraptor* [15, 45]. Furthermore, the wing shape of *Microraptor* differs from shorebird, waterbird, and falcon wing shapes, particularly with its proportionally large non-manus wing portion (arm-wing) compared to its relatively slender manus wing portion (hand-wing) forming the V-shaped wingtip. This suggests that there is more drag produced by the hand-wing than the arm-wing and a need for greater proportional thrust production (sensu Durmus [110]), indicating a lower flight speed regime than modern analogues. Finally, falcons also possess a range of traits common to modern birds that *Microraptor* lacks (e.g., sternal keels and triosseal canals), many of which improve upstroke speed and, consequently, overall flight performance (see *Deltopectoral crest and flapping versus non-flapping flight* for further discussion).

Beyond anatomical differences, there are also habitat disparities between *Microraptor* and modern analogues, i.e., shorebirds, waterbirds and falcons. The latter are overwhelmingly residents of open habitats, while *Microraptor* specimens are known from areas forested by gymnosperm-dominated floras [111]. Modern birds living in cluttered habitats tend to have moderately slotted wingtips, including aerial pursuit predators such as hawks and sparrowhawks (*Accipiter* genus). However, *Microraptor* lacks wingtip slotting. We speculate that microraptorine feather anatomy may have been incompatible with wingtip slotting because of the absence of free-edge trailing vanes in the feathers (see Feo et al. [56]), but this needs to be further explored.

In short, *Microraptor* possessed a wing shape with no 'perfectly' matching modern analogue, similar to what has been observed in *Confuciusornis* [8]. That said, the use of modern analogue wing shapes does provide us with context for comparison to other paravians of the Late Jurassic to Early Cretaceous, particularly *Archaeopteryx* and *Anchiornis*. In comparison to the latter taxa, the wings of *Microraptor* appear comparatively specialised to high speed and agility. This comports with other current evidence from the foot morphology [33] and preserved meals [24, 103–105]. The total evidence, including wing shape, in comparison with contemporary avians and basal avialans, broadly suggests that *Microraptor* was a moderately-fast, high-agility, flying forager engaging in short-range ambush within cluttered environments.

Radial biceps tuberosity and foraging behaviour

The presence of a prominent biceps tuberosity in *Microraptor* (also mentioned as the bicipital tubercule in the literature [112–114]) suggests that it developed a strong attachment for a strong biceps muscle, as seen in several early avialans including the early pygostylian *Sapeornis*, the enanthiornine *Mirusavis*, and the ornithurines *Yanornis* and *Yixianornis* [112–114]. In modern falcons like peregrines (*Falco peregrinus*) and merlins (*Falco columbarius*), M. biceps brachii is an important muscle of the flexor/stabiliser group which is used to rapidly change wing position and hold the wing fixed to increase velocity during the stoop to catch prey [102]. However, it is worth noting that the wing bones of stooping falcons, especially peregrines (*Falco peregrinus*), are particularly adapted to torsion and bending [115]. Analysis of the humeral structural strength of *Microraptor* specimen IVPP V13352 showed that the humerus was strong enough to support sustained flight [116], but the reported section modulus is only a small fraction of that reported for stooping falcons [83], suggesting that the humerus of *Microraptor* would not support the forces required for stoop hunting. As M. biceps brachii is important for changing and stabilising the wing position during stooping in falcons, it is also important for keeping the wing in position during flight in specialised gliding and soaring modern birds [117]. Thus, we hypothesise that *Microraptor* had a well-developed and strong flexor/stabiliser potentially improving inferred pursuit predation performance by enabling it to swiftly change wing positions and was also an important component to steady its wing during aerodynamic stress in flight. The strong flexor/stabiliser in *Microraptor* is also supported by the relatively large shoulder soft tissue profile that is seen in specimen STM 5–221 [12]. It should be noted that *Microraptor* has been suggested as an arboreal animal [21, 118, 119] and a stronger M. biceps brachii combined with its highly curved manus claws could also have been an advantage for climbing, or at least grapple from tree trunks or branches (however see next section for further discussion: *Manus claws and arboreality*).

Manus claws and arboreality

Ecology is hard to infer based on claw curvature (manus and pes) alone as claws can have different functions [120, 121]. Manual phalangeal index (phalanges length: metacarpal length; phalanges length excluding unguals sensu Dececchi and Larsson [122]) is considered to be a good indicator of arboreality in mammals [123]. Claw and grip-based climbing are expected to have enlarged phalangeal indices [124, 125] but the index of *Microraptor* is low compared to other theropods [122]. However, the juvenile hoatzin bird is able to climb in densely packed and narrow-radius branches with a similar phalangeal index to *Microraptor* and claws that are less recurved and broader than *Microraptor* (including with claw sheaths; Tables S5 and S6 in Additional file 1). Thus, *Microraptor* might have had manual claws that were less resistant to supporting climbing forces compared to juvenile hoatzin. The more recurved and slender claws of *Microraptor* may potentially be more of legacy of its dromaeosaurid ancestry than an adaptation for climbing function. Thus, it remains difficult to constrain the degree of arboreality in *Microraptor* with pes claw curvature emphasising this uncertainty (see Chotard et al. [47] for discussion on pes claw curvature). A more satisfying answer to this question may lie in future work using additional lines of evidence like FEA (Finite Element Analysis) and range of motion. For example, FEA of a manus claw of *Velociraptor* suggested it was able to support its own weight while climbing [126]. Also, a range of motion study would give insight into the forearm positions available to *Microraptor*, helping to distinguish whether climbing motions or hanging postures were possible, while keeping in mind the potential movement restrictions necessary to limit damage to the long feathers of the forewing and hindwing.

Distal carpal 3, a functional pisiform/ulnare analogue of modern birds?

The radiale and semilunate system indicate high flexibility in the wrist of *Microraptor.* This would have allowed the hand to be folded back, moving attached feathers from a ventral to posterior orientation so that the wing could be tucked safely alongside the body [127]. Distal carpal 3 in specimen STM 5–75 is in the same position as the 'pisiform' in modern birds (name suggested by Botelho et al. [75] to differentiate the modern bird ulnare from the non-avialan dinosaur ulnare as they argued they are different bones), suggesting distal carpal 3 may have the same function as the 'pisiform'. Modern birds use the 'pisiform' during the downstroke to transmit force between the ulna and the carpometacarpus and use it during the upstroke to restrict wing flexibility [75]. The ulnare was lost in early dinosaurs and the 'pisiform' appeared in early avialans [75, 92]. Distal carpal 3 (labelled distal carpal 4 in Xu et al. [76]) has been identified in early dinosaurs and in many theropods, including paravians [75, 76]. Xu et al. [76] suggested that this distal carpal is present in earlier ontogenetic stages and fuses with the 'large medial distal carpal' (semilunate) in some adult deinonychosaurians, including *Microraptor* specimens IVPP V17749 and V17750. The largest *Microraptor* we studied that preserves a semilunate and distal carpal 3 is STM 5–93 (0.98 kg) and these carpals are not fused. In such cases, a pisiform-like function of distal carpal 3 is expected to have improved flight performance, which future simulation work can help to test.

Role of manus osteology, musculature, and feather structure in wing shape control

The presence of a long and broad digit II in *Microraptor* presumably helped to support the attachment points of the primary remiges, which are attached on the dorsoposterior side of digit II in modern flying birds [19, 96, 128]. As there was no separation between digits II and III (STM 5–221, Fig. 9), *Microraptor* could have had a functional didactyl hand as previously suggested for *Anchiornis* and Enantiornithes [34, 97]. A functional didactyl hand would not limit the effectiveness of *Microraptor* to secure prey or to grab a vertical substrate, as dromaeosaurid prehensile behaviour would favour flexed wrists to avoid supination of the hand during wrist extension and contact between the wings, while keeping prey between the palms [129]. In addition, a broader second digit and accolated third digit offers more surface area for muscles and soft tissues to attach sturdily and deeply embed calami into the postpatagium [8, 130], as can be seen in enantiornithines and confuciusornithiforms [97, 131]. As *Microraptor* combines all of these traits — broad digit II, accolated digits II and III, large postpatagium, and deeply embedded calami — it appears to have had significant control over the cohesiveness of its wing shape and thus an aerofoil well-adapted to aerodynamic (especially aeroelastic) stresses, as in modern birds. In contrast, *Anchiornis* does not have a large postpatagium and deeply embedded calami [34], indicating a less cohesive wing than *Microraptor* and modern birds. As the postpatagium is also responsible for generating lift, though not as much as the propatagium [132], *Microraptor* would also gain a performance benefit from the enlarged and better stabilised postpatagium.

Deltopectoral crest and flapping versus non-flapping flight

Serrano and Chiappe [133] reported a distinction in modern birds between species that predominantly utilise soaring and those that predominantly utilise flapping flight. This distinction is apparent when comparing the size of the deltopectoral crest relative to body size (with the deltopectoral crest being longer relative to body size in soaring specialists). They suggest that this relationship exists based on lever theory, implying that for a given body mass and regardless of wingspan, a shorter deltopectoral crest has advantages for flapping the wing faster. This could also reflect the modification in the "gearing" of the wing-muscle system in soaring modern birds, trading off some wingbeat speed for out-lever force to balance the energy needed to take-off with flapping and the energy needed to maintain the wing in soaring position. Using this relationship and aerodynamic models, Serrano and Chiappe [133] suggested *Sapeornis* utilised thermal soaring. Applying this relationship to *Microraptor*, specimens from our study plot closer to modern birds with flapping flight, and much lower than *Sapeornis* specimens which plot closer to modern birds with soaring flight (Fig. S6 in Additional file 2). This suggests that *Microraptor* has a deltopectoral crest associated with higher frequency wingbeat cycles than *Sapeornis*. Thus, *Microraptor* could utilise its proportionally shorter deltopectoral crest to flap its wings more efficiently using less energy than *Sapeornis*, which itself seems to be using soaring as its energy efficient flight behaviour (i.e., less flapping sensu Pennycuick [134] and Butler [135]). This is associated with the development of shoulder muscles and sternal internal bone structure showing flight-related loading in *Microraptor* [11]. Altogether and with the suggested wing posture of early non-avialan paravians and the potentially more anterodorsal-posteroventral wing movements of at least some taxa [12, 79, 136, 137], *Microraptor* could have developed some degree of active flight. However, there are differences between the flight apparatus of fossil and modern birds [12, 136–138]. In the case of *Microraptor*, its sternum lacks a keel [12] and it lacks a fully or partially closed triosseal canal [77, 79, 139], which enables the upstroke to be powered by expanded ventral musculature in ornithothoracine birds [139, 140]. The carpal and metacarpal bones of *Microraptor* are free compared to the fully fused carpometacarpus of modern birds. The carpometacarpus precursor only appeared in early pygostylian birds before further fusion occurred among enantiornithines and ornithuromorphs [141, 142]. The flapping flight of modern birds is improved by the fully fused carpometacarpus and the specialised carpals (radiale and ulnare) which avoid hyperpronation during the upstroke and supination during the downstroke [143]. Despite these differences, *Microraptor* possesses features that could fill the roles above or provide alternative solutions. In contrast to the "pulley-system" of modern birds, *Microraptor* has well-developed shoulder muscles with presumably a shoulder-powered upstroke as suggested by the oriented linear internal structure of its sternum and preserved soft tissues revealed under LSF [12]. The *Microraptor* flight muscle complex is functionally closer to that seen in bats, although the anatomy is also different. Active flight in bats is powered by muscles of the shoulder, back, and chest. Their sternum is reduced and segmented, as in all mammals [144], and though the manubrium often possesses a keel, it is much smaller than the long and fused sternal keel of birds. Bats also have no structure analogous to the triosseal canal. Instead, their upstroke is powered by the shoulder and extrinsic back [145, 146]. This system is equally capable of specialising to high-speed, high agility flight, as evidenced by recorded speeds of open-air flying bats that match or exceed those measured for any similar-sized birds [147]. If we take a closer look at the wrist and manus, although *Microraptor*'s wrist has a higher degree of freedom with the semilunate not fused to the metacarpals, the radiale and distal carpal 3 could have the same functions as the radiale and ulnare of modern birds to some extent. Thus, the kinematics of potential active flight in *Microraptor* would be different from modern birds, although similar flight dynamics can be found between them. In the context of early evolution of flight, it is important to keep in consideration that different functional pathways may exist to achieve similar locomotor behaviours [138], especially considering the aerodynamic role of the hindwings of *Microraptor* (see Hefler et al. [148] and Chotard et al. [47]).

Ulna-humerus length ratio and flight capability

Flight characteristics can be correlated with the ulna:humerus or radius:humerus length ratios. In the data from Wang et al. [149], modern birds with longer ulnae are birds with aquatic lifestyles and migratory behaviours or that only use flight when startled (burst flight). The *Microraptor* specimens have ulna:humerus ratios that are similar to modern birds with longer ulnae (Table S7 in Additional file 1), including long-distance migratory flyers (as in waterbirds with such ratios) and burst flight/aerial sprinting flyers. The latter of these would be more consistent with other anatomical features of *Microraptor*, including foot morphology [33], a prominent biceps tuberosity indicating an aerial hunting lifestyle and a deltopectoral crest associated with 'high' frequency wingbeat cycles. Comparing the new radius:humerus length ratio of *Microraptor* (~ 0.8 to ~ 1.0) with data from Benson and Choiniere [86] and Middleton and Gatesy [87], the ratio of *Microraptor* was found to fall between the ratios of non-flying modern birds (~ 0.4 to ~ 1.1) and flying modern birds (~ 0.8 to ~ 1.4), but close to the ratios for fossil avialans (~ 0.8 to ~ 1.2) (Table S8 in Additional file 1). Intermediate values for limb proportions between non-flyers and flyers can also be seen in the early evolution of bats as evident from *Onychonycteris*. Although *Onychonycteris* has the same skeletal features for powered flight as other bats, its limb proportions fall in between those of forelimb-dominant non-flying mammals and those of Eocene and modern bats [150]. This shows that these forelimb anatomical correlates seen in modern animals cannot be solely used to determine ancient flight capabilities (see Lowi-Merri et al. [49] and Akeda and Fujiwara [151]).

Early evolution of contour feathering

The presence of anteriorly and dorsally projecting marginal coverts suggest that the propatagium of *Microraptor* was well adapted to maintain a cambered profile [67] and to supplement the lift generated by the remiges [132], as seen in Confuciusornithiformes and modern flying birds [131]. Modern type contour feathers were previously suggested to be an exclusive feature of avialans [4], but marginal covert features of *Microraptor* now suggest that they have a deeper origin among early paravians. It cannot yet be ruled out that this feather type evolved more than once within Paraves.

Early alula evolution

In modern birds, the alula feathers function as vortex generators to increase lift control and enhance flight manoeuvrability, especially in low-speed flight (such as on landing approach) [152, 153]. Our new observations of *Microraptor* did not identify alula feathers (*contra* Xu et al. [21], Ksepka [154]) or an alular patagium. Similar to IVPP V13352, specimen STM 5–172 has feathers around digit I projecting from metacarpal II and are thus marginal coverts that have been displaced. However, as these feathers are clumped together, we cannot rule out that alula feathers might be hidden among them (Fig. S5B in Additional file 2). Future discoveries and descriptions of hand feathering in *Microraptor* would be invaluable in testing whether *Microraptor* had alula feathers and assessing their associated flight advantages. For example, the *Microraptor* specimen QM V1002 has feathers on the anterior side of its right digit I which have not been described [24], but they seem to have a strange projecting angle compared to the manus, so further inspection of the specimen would be worthwhile. The early bird *Eoconfuciusornis* possesses alular feathering but is missing an alular patagium [131], so it is important to note that when studying early alula evolution, the absence of an alular patagium does not necessarily rule out the presence of an alula.

Conclusions

Recent studies suggest that *Microraptor* had greater flight capabilities than previously thought [12, 13] and was more than just an 'ineffective' glider [14]. This is also supported by our revision and description of the forelimb and forewing anatomy of historic and new specimens, which provides additional evidence of *Microraptor*'s adaptations for a more complex flight behaviour. Extant gliders tend to have low aspect ratio "wings" (although it is not the only aspect that controls gliding capabilities) [31, 155–157]. In contrast, the wing of *Microraptor* has a high aspect ratio and its shape, although unique, is closest to wing shapes seen in modern falcons, shorebirds and waterbirds. Moderate to strong aerial capabilities are supported by the anatomical features providing wing cohesiveness as well as a wing structure with both leading-edge flexibility and resistance to aerodynamic stress in *Microraptor*: a large propatagium and postpatagium, broad digit II, accolated digit II and III, deeply embedded calami, and strong flexor/stabiliser group. The strong flexor/stabiliser group in the upper arm inferred from its prominent biceps tuberosity and soft tissue profile also suggests that *Microraptor* was an aerial hunter capable of aerial pursuit and ambushing. This raptorial lifestyle and flight dynamics are congruent with previous suggestions based on specialised foot-morphology [33]. Deltopectoral crest morphology and lever theory (sensu Serrano and Chiappe [133]) is congruent with soft tissues preserved in the shoulder and the internal linear bone structure of the sternum of *Microraptor* [12], suggesting it might have been capable of some degree of active flight, but with different flapping kinematics than seen in extant birds. Regarding the lifestyle of *Microraptor* as an arboreal animal [22, 118, 119], the strong M. biceps brachii could be new evidence supporting the ability for trunk hanging or climbing, but the highly recurved and relatively slender claws of *Microraptor* do not match the rather broad and less recurved claw of juvenile hoatzin birds. This suggests that the claws of *Microraptor* are potentially a characteristic more of their dromaeosaurid heritage rather than an arboreality adaptation. There is still missing information about the presence or absence of alula feathers, the shape of the tertiary feathers (humeral feathers), and the identification and role of the distal carpal 3, which all have implications on its flight behaviour that should be followed up on in future work. However, along with the new elements described in this study, we can already see multiple features suggesting 'advanced' flying capabilities, supporting *Microraptor* as a moderately-fast flyer foraging with short-range ambushes in cluttered environments, in comparison to other early paravians. In avialans, there is a good record of different stages of the flight evolution starting with early members with less aerodynamically refined wings (e.g. *Anchiornis* [13, 158]). However, in dromaeosaurids, we are still lacking information on the earliest stages of flight evolution. The flight-related features described in our study have not yet been described in other microraptorines preserving feathers (see *Sinornithosaurus* [159], *Tianyuraptor* [71], *Changyuraptor* [91], *Zhenyuanlong* [55], *Wulong* [57]) and many dromaeosaurids do not preserve direct evidence of soft tissues or feathers (e.g., *Dromaeosaurus* [160], *Achillobator* [161], *Bambiraptor* [162]). Future discoveries and more precise description of dromaeosaurids would therefore be especially important if we are to deepen our understanding of how dromaeosaurid evolved flight in parallel to avialans, and their role in the broader landscape of theropod flight evolution. It should not be forgotten that many of the early paravians possess not one pair of wings but two, including *Microraptor*, which need to be considered carefully when studying flight in these animals (see Chotard et al. [47]). Although modern birds are considered to be the best analogue, it cannot be ignored that different body plans could lead to similar functions and behaviours [138]. Further aerodynamic modelling of *Microraptor* building on past work using the new insights gained in this study would also be important in this goal [148]. These future studies on *Microraptor* can utilise the new information from this exhaustive description of the forelimb and test the hypotheses when performing integrative studies including its hindwings and/or tail. This study underscores the ongoing legacy of Chinese feathered dinosaurs in studying theropod flight evolution, the importance of utilising larger specimen samples that include specimens preserving different features of the animal, and new technologies to obtain new insights.

Supplementary Information

The online version contains supplementary material available at https://doi.org/10.1186/s12862-025-02397-5.

Additional file 1. Contains additional tables with different measurements and ratios taken from the *Microraptor* specimens of this study to compare with other paravians.

Additional file 2. Contains the figures of additional specimens that were described in the text and the figure of the OLS regression used to test the flight behaviour of *Microraptor*.

Acknowledgements

The attendees of the 2nd International Pennaraptoran Dinosaur Symposium at The Chinese University of Hong Kong (IPDS2) and the symposium 'Theropod Flight Origins: Latest Insights and New Frontiers' at the 83rd Annual Meeting of the Society of Vertebrate Paleontology in Cincinnati are thanked for their feedback and suggestions. The authors also thank Binghe Geng (IVPP), Dawei Zhang and Xiaomei Zhang (STM) for facilitating the study of specimens in their care.

Authors' contributions

MP, TGK, XLW and XTZ conceived and designed the experiment. MG, XLW, XTZ, TGK, MC, LAB, TAD, MBH, JZ, SAH, XX & MP acquired the data. MG, XLW, XTZ, TGK, MC, LAB, TAD, MBH, JZ, SAH, XX & MP analysed the data. MG, XLW, XTZ, TGK, MC, LAB, TAD, MBH, JZ, XX & MP interpreted the data. MG, XLW, XTZ, MC, LAB, TGK, TAD, MBH, JZ & MP drafted the manuscript. All authors read, revised and approved the final manuscript.

Funding

MP's, TGK's, XLW's and XTZ's participation in the study was supported by the Research Grant Council of Hong Kong's General Research Fund (17120920; 17103315; 14116623; 14113824), including MG's and MC's participation via Research Assistant and PhD student roles and LAB's participation via a Research Assistant role. MP, MG and MC were also supported by the Faculty of Science and School of Life Sciences of The Chinese University of Hong Kong, including a Postgraduate Scholarship (CUHK PGS) for MG and MC. XLW and XTZ were also supported by the Taishan Scholar Foundation of Shandong Province (Ts20190954 to XLW) and the National Natural Science Foundation of China (42288201 to XLW). XX was supported by the National Natural Science Foundation of China (Grant No. 42288201) and Yunnan Revitalization Talent Support Program (202305AB350006).

Data availability

The datasets supporting the conclusions of this article are included within the article (and its additional files).

Declarations

Ethics approval and consent to participate

Not applicable.

Consent for publication

Not applicable.

Competing interests

Michael Pittman, T. Alexander Dececchi & Michael B. Habib are guest editors for the Vertebrate Flight Evolution collection and should not be considered for editorial duties for this manuscript. No other authors declare competing interest.

Author details

[1]School of Life Sciences, The Chinese University of Hong Kong, Shatin, Hong Kong SAR, China. [2]Institute of Geology and Paleontology, Linyi University, Linyi City, Shandong 276005, China. [3]Shandong Tianyu Museum of Nature, Pingyi, Shandong 273300, China. [4]Foundation for Scientific Advancement, Sierra Vista, AZ 85650, USA. [5]Division of Natural Sciences, Dakota State University, Madison, SD, USA. [6]David Geffen School of Medicine, University of California Los Angeles, Los Angeles, CA, USA. [7]School of Life and Environmental Sciences, College of Health and Sciences, University of Lincoln, Brayford Pool Campus, Lincoln, UK. [8]Department of Integrative Biology, University of Wisconsin-Madison, Madison, WI 53706, USA. [9]Centre for Vertebrate Evolutionary Biology, School of Life Sciences, Yunnan University, Chenggong, Kunming 650504, China. [10]Key Laboratory of Vertebrate Evolution and Human Origins, Institute of Vertebrate Paleontology and Paleoanthropology, Chinese Academy of Sciences, Beijing 100044, China.

Received: 16 October 2024 Accepted: 20 May 2025
Published online: 01 July 2025

References

1. Norberg UM. Flying, gliding, and soaring. Functional vertebrate morphology. Cambridge: Harvard University Press; 2013. pp. 129–58.
2. Baliga VB, Szabo I, Altshuler DL. Range of motion in the avian wing is strongly associated with flight behavior and body mass. Sci Adv. 2019;5(10):eaaw6670.
3. Longrich NR, Vinther J, Meng QJ, Li QG, Russell AP. Primitive wing feather arrangement in *Archaeopteryx lithographica* and *Anchiornis huxleyi*. Curr Biol. 2012;22(23):2262–7.
4. Saitta ET, Gelernter R, Vinther J. Additional information on the primitive contour and wing feathering of paravian dinosaurs. Palaeontology. 2018;61(2):273–88.
5. Lefèvre U, Cau A, Hu D, Godefroit P. Feather evolution in Pennaraptora. In: Foth C, Rauhut OWM, editors. The evolution of feathers: from their origin to the present. Cham: Springer International Publishing; 2020. p. 103–18.
6. O'Connor J. The plumage of basal birds. In: Foth C, Rauhut OWM, editors. The evolution of feathers: from their origin to the present. Cham: Springer International Publishing; 2020. p. 147–72.
7. Pittman M, Heers AM, Serrano FJ, Field DJ, Habib MB, Dececchi TA, Kaye TG, Larsson BCE. Methods of studying early theropod flight. B Am Mus Nat Hist. 2020;440:277–94.
8. Falk AR, Kaye TG, Zhou Z, Burnham DA. Laser fluorescence illuminates the soft tissue and life habits of the Early Cretaceous bird *Confuciusornis*. PLoS ONE. 2016;11(12): e0167284.
9. Zheng XT, Zhou ZH, Wang XL, Zhang FC, Zhang XM, Wang Y, Wei GJ, Wang S, Xu X. Hind wings in basal birds and the evolution of leg feathers. Science. 2013;339(6125):1309–12.
10. Pei R, Li QG, Meng QJ, Gao KQ, Norell MA. A new specimen of *Microraptor* (Theropoda: Dromaeosauridae) from the Lower Cretaceous of western Liaoning. China Am Mus Novit. 2014;3821:1–28.
11. Li QG, Gao KQ, Meng QJ, Clarke JA, Shawkey MD, D'Alba L, Pei R, Ellison M, Norell MA, Vinther J. Reconstruction of *Microraptor* and the evolution of iridescent plumage. Science. 2012;335(6073):1215–9.
12. Pittman M, Kaye TG, Wang X, Zheng X, Dececchi TA, Hartman SA. Preserved soft anatomy confirms shoulder-powered upstroke of early theropod flyers, reveals enhanced early pygostylian upstroke, and explains early sternum loss. P Natl Acad Sci. 2022;119(47): e2205476119.
13. Pei R, Pittman M, Goloboff PA, Dececchi TA, Habib MB, Kaye TG, Larsson HCE, Norell MA, Brusatte SL, Xu X. Potential for powered flight neared by most close avialan relatives, but few crossed its thresholds. Curr Biol. 2020;30(20):4033-+.
14. Dyke G, de Kat R, Palmer C, van der Kindere J, Naish D, Ganapathisubramani B. Aerodynamic performance of the feathered dinosaur Microraptor and the evolution of feathered flight. Nat Commun. 2013;4:4.
15. Dececchi TA, Larsson HCE, Habib MB. The wings before the bird: an evaluation of flapping-based locomotory hypotheses in bird antecedents. Peerj. 2016;4:e2159.
16. Shahid F, Zhao J-S, Godefroit P. Design of flying robots inspired by the evolution of avian flight. Proc Inst Mech Eng Pt C J Mechan Eng Sci. 2019;233(23–24):7669–86.
17. Pittman M, O'Connor J, Tse E, Makovicky P, Field DJ, Ma W, Turner AH, Norell MA, Pei R, Xu X. The fossil record of Mesozoic and Paleocene pennaraptorans. Bull Am Mus Nat Hist. 2020;440:37–96.
18. Wang R, Pei R. The smallest known specimen of Microraptor (Dinosauria: Dromaeosauridae) from the Jiufotang Formation in northeastern China. Hist Biol. 2024:1–11.
19. Gong E-P, Martin LD, Burnham DA, Falk AR, Hou L-H. A new species of *Microraptor* from the Jehol Biota of northeastern China. Palaeoworld. 2012;21(2):81–91.
20. Turner AH, Makovicky PJ, Norell MA. A review of dromaeosaurid systematics and paravian phylogeny. B Am Mus Nat Hist. 2012;371:5–206.
21. Xu X, Zhou ZH, Wang XL, Kuang XW, Zhang FC, Du XK. Four-winged dinosaurs from China. Nature. 2003;421(6921):335–40.
22. Xu X, Zhou ZH, Wang XL. The smallest known non-avian theropod dinosaur. Nature. 2000;408(6813):705–8.
23. Senter P, Barsbold R, Britt B, Burnham D. Systematics and evolution of Dromaeosauridae (Dinosauria, Theropoda). Bull Gunma Mus Natu. 2004;8:1–20.
24. Xing L, Persons Iv WS, Bell PR, Xu X, Zhang J, Miyashita T, Wang F, Currie PJ. Piscivory in the feathered dinosaur *Microraptor*. Evolution. 2013;67(8):2441–5.
25. Featherbase. Haase A, Schlusen J, Schwenk K. https://www.featherbase.info/uk/home. Accessed 8 July 2024.
26. Vogelfedern - die Seite als Bestimmungshilfe für Mauserfedern und Rupfungen. Schubert, S. http://www.vogelfedern.de/index-e.htm. Accessed 8 July 2024.

27. Puget sound museum, wing and tail image collection. https://www.jstor.org/site/pugetsound/wing-and-tail-image-collection/. Accessed 13 Dec 2024.
28. Ramanujan K. Research museum secures rare California condors. Cornell CALS: Ithaca, NY; 2018. https://cals.cornell.edu/news/research-museum-secures-rare-california-condors. Accessed 8 July 2024.
29. Division of Birds Collections. Smithsonian National Museum of Natural History. https://collections.nmnh.si.edu/search/birds/. Accessed 8 July 2024.
30. Kaye TG, Falk AR, Pittman M, Sereno PC, Martin LD, Burnham DA, Gong EP, Xu X, Wang YN. Laser-stimulated fluorescence in paleontology. Plos One. 2015;10(5):e0125923.
31. Dececchi TA, Roy A, Pittman M, Kaye TG, Xu X, Habib MB, Larsson HCE, Wang XL, Zheng XT. Aerodynamics show membrane-winged theropods were a poor gliding dead-end. Iscience. 2020;23(12):101574.
32. Kaye TG, Pittman M, Wahl WR. *Archaeopteryx* feather sheaths reveal sequential center-out flight-related molting strategy. Commun Biol. 2020;3(1):745.
33. Pittman M, Bell PR, Miller CV, Enriquez NJ, Wang X, Zheng X, Tsang LR, Tse YT, Landes M, Kaye TG. Exceptional preservation and foot structure reveal ecological transitions and lifestyles of early theropod flyers. Nat Commun. 2022;13(1):7684.
34. Wang XL, Pittman M, Zheng XT, Kaye TG, Falk AR, Hartman SA, Xu X. Basal paravian functional anatomy illuminated by high-detail body outline. Nat Commun. 2017;8:8.
35. Xu X, Zhou ZH, Dudley R, Mackem S, Chuong C-M, Erickson GM, Varricchio DJ. An integrative approach to understanding bird origins. Science. 2014;346(6215):1253293.
36. Towers M, Signolet J, Sherman A, Sang H, Tickle C. Insights into bird wing evolution and digit specification from polarizing region fate maps. Nat Commun. 2011;2(1):426.
37. Kawahata K, Cordeiro IR, Ueda S, Sheng G, Moriyama Y, Nishimori C, Yu R, Koizumi M, Okabe M, Tanaka M. Evolution of the avian digital pattern. Sci Rep-Uk. 2019;9(1):8560.
38. Pike AVL, Maitland DP. Scaling of bird claws. J Zool. 2004;262(1):73–81.
39. Foth C. On the identification of feather structures in stem-line representatives of birds: evidence from fossils and actuopalaeontology. Palaontol Z. 2012;86(1):91–102.
40. Clark GAJ. Integumentum commune. In: Baumel JJ, King AS, Breazile JE, Evans HE, Vanden Berge JC, editors. Handbook of avian anatomy: Nomina Anatomica Avium. Publications of the Nuttall Ornithological Club. Second Edition ed. Cambridge, Massachusettes: The Club; 1993. p. 17 - 44.
41. Morlion ML. Pterylosis of the wing and tail in the noisy scrubbird *Atrichornis clamosus*, and superb lyrebird *Menura novaehollandiae* (Passeriformes: Atrichornithidae and Menuridae). Rec Aust Mus. 1985;37:143–56.
42. Benson RBJ, Hunt G, Carrano MT, Campione N. Cope's rule and the adaptive landscape of dinosaur body size evolution. Palaeontology. 2018;61(1):13–48.
43. Campione NE, Evans DC, Brown CM, Carrano MT. Body mass estimation in non-avian bipeds using a theoretical conversion to quadruped stylopodial proportions. Methods Ecol Evol. 2014;5(9):913–23.
44. Turner AH, Pol D, Clarke JA, Erickson GM, Norell MA. A basal dromaeosaurid and size evolution preceding avian flight. Science. 2007;317(5843):1378–81.
45. Allen V, Bates KT, Li Z, Hutchinson JR. Linking the evolution of body shape and locomotor biomechanics in bird-line archosaurs. Nature. 2013;497(7447):104–7.
46. Dececchi TA, Larsson HCE, Pittman M, Habib M. High flyer or high fashion? A comparison of flight potential among small bodied paravians. Bull Am Mus Nat Hist. 2020;440:295–320.
47. Chotard M, Wang X, Zheng X, Kaye TG, Grosmougin M, Barlow L, Kundrát M, Dececchi TA, Habib MB, Zariwala J, Hartman S, Xu X, Pittman M. New information on the Hind limb feathering, soft tissues and skeleton of *Microraptor* (Theropoda: Dromaeosauridae). BMC Ecol Evo. 2025;25(1):37.
48. Lovette I, Fitzpatrick J. Handbook of bird biology. 3rd ed. Ithaca: Cornell University Press; 2016.
49. Lowi-Merri TM, Benson RBJ, Claramunt S, Evans DC. The relationship between sternum variation and mode of locomotion in birds. BMC Biol. 2021;19(1):165.
50. Tobalske BW, Dial KP. Aerodynamics of wing-assisted incline running in birds. J Exp Biol. 2007;210(10):1742–51.
51. Savile DBO. Adaptive evolution in the avian wing. Evolution. 1957;11(2):212–24.
52. Durmuş S. Investigation of wing forms through mass and wing area chart. Turk J Nat Sci. 2022;11(2):107–12.
53. Kumar MH, Dorlikar P. Analysis of elliptical wing type bird inspired device. IOP Conf Ser: Mater Sci Eng. 2021;1116(1): 012147.
54. Tobalske BW, Dial KP. Effects of body size on take-off flight performance in the Phasianidae (Aves). J Exp Biol. 2000;203(21):3319–32.
55. Lü JC, Brusatte SL. A large, short-armed, winged dromaeosaurid (Dinosauria: Theropoda) from the Early Cretaceous of China and its implications for feather evolution. Sci Rep-Uk. 2015;5:5.
56. Feo TJ, Field DJ, Prum RO. Barb geometry of asymmetrical feathers reveals a transitional morphology in the evolution of avian flight. P Roy Soc B: Biol Sci. 2015;282(1803):20142864.
57. Poust AW, Gao CL, Varricchio DJ, Wu JL, Zhang FJ. A new microraptorine theropod from the Jehol Biota and growth in early dromaeosaurids. Anat Rec. 2020;303(4):963–87.
58. Hu D, Hou L, Zhang L, Xu X. A pre-*Archaeopteryx* troodontid theropod from China with long feathers on the metatarsus. Nature. 2009;461(7264):640–3.
59. Kiat Y, Balaban A, Sapir N, O'Connor JK, Wang M, Xu X. Sequential molt in a feathered dinosaur and implications for early paravian ecology and locomotion. Curr Biol. 2020;30(18):3633-+.
60. Jukema J, van de Wetering H, Klaassen RHG. Primary moult in non-breeding second-calendar-year swifts *Apus apus* during summer in Europe. Ring Migr. 2015;30(1):1–6.
61. Laysan albatross, 10908a, male, Jul. Wing and tail image collection. University of Puget Sound. https://jstor.org/stable/community.36062164. Accessed 8 Nov 2024.
62. Laysan albatross, 21460a, female, Dec. Wing and tail image collection. University of Puget Sound. https://jstor.org/stable/community.36062166. Accessed 8 Nov 2024.
63. Rock pigeon, 11000a, female, Apr. Wing and tail image collection. University of Puget Sound. https://jstor.org/stable/community.36064819. Accessed 8 Nov 2024.
64. Rock pigeon, 17193a, male, Apr. Wing and tail image collection. University of Puget Sound. https://jstor.org/stable/community.36062753. Accessed 8 Nov 2024.
65. Rock pigeon, 20721a, female, Apr. Wing and tail image collection. University of Puget Sound. https://jstor.org/stable/community.36064832. Accessed 8 Nov 2024.
66. Li QG, Clarke JA, Gao KQ, Peteye JA, Shawkey MD. Elaborate plumage patterning in a Cretaceous bird. Peerj. 2018;6:6.
67. Brown RE, Baumel JJ, Klemm RD. Anatomy of the propatagium: the great horned owl (*Bubo virginianus*). J Morphol. 1994;219(2):205–24.
68. Hu DY, Clarke JA, Eliason CM, Qiu R, Li QG, Shawkey MD, Zhao CL, D'Alba L, Jiang JK, Xu X. A bony-crested Jurassic dinosaur with evidence of iridescent plumage highlights complexity in early paravian evolution. Nat Commun. 2018;9:217.
69. Hwang SH, Norell MA, Qiang J, Gao KQ. New specimens of *Microraptor zhaoianus* (Theropoda : Dromaeosauridae) from northeastern China. Am Mus Novit. 2002;3381:1–44.
70. Xu X, Qin Z. A new tiny dromaeosaurid dinosaur from the Lower Cretaceous Jehol Group of western Liaoning and niche differentiation among the Jehol dromaeosaurids. Vert PalAs. 2017;55(2):129–44.
71. Zheng X, Xu X, You H, Zhao Q, Dong Z. A short-armed dromaeosaurid from the Jehol Group of China with implications for early dromaeosaurid evolution. P Roy Soc B: Biol Sci. 2010;277(1679):211–7.
72. Pei R, Li QG, Meng QJ, Norell MA, Gao KQ. New specimens of *Anchiornis huxleyi* (Theropoda: Paraves) from the Late Jurassic of northeastern China. B Am Mus Nat Hist. 2017;411:4–66.
73. Chiappe LM, Shu'an J, Qiang J, Norell MA. Anatomy and systematics of the Confuciusornithidae (Theropoda : Aves) from the late mesozoic of northeastern China. B Am Mus Nat Hist. 1999;242:3–89.
74. Navalón G, Meng QJ, Marugán-Lobón J, Zhang YG, Wang BP, Xing H, Liu D, Chiappe LM. Diversity and evolution of the Confuciusornithidae: evidence from a new 131-million-year-old specimen from the Huajiying Formation in NE China. J Asian Earth Sci. 2018;152:12–22.

75. Botelho JF, Ossa-Fuentes L, Soto-Acuna S, Smith-Paredes D, Nunez-Leon D, Salinas-Saavedra M, Ruiz-Flores M, Vargas AO. New developmental evidence clarifies the evolution of wrist bones in the dinosaur-bird transition. Plos Biol. 2014;12(9):e1001957.
76. Xu X, Han FL, Zhao Q. Homologies and homeotic transformation of the theropod "semilunate" carpal. Sci Rep-Uk. 2014;4:4.
77. Wu Q, O'Connor JK, Wang SY, Zhou ZH. Transformation of the pectoral girdle in pennaraptorans: critical steps in the formation of the modern avian shoulder joint. Peerj. 2024;12:12.
78. Kassem MAM, Tahon RR, Khalil KM, El-Ayat MA. Morphometric studies on the appendicular bony skeleton of the ostriches (*Struthio camelus*). BMC Vet Res. 2023;19(1):109.
79. Novas FE, Motta MJ, Agnolín FL, Rozadilla S, Lo Coco GE, Brissón Egli F. Comments on the morphology of basal paravian shoulder girdle: new data based on unenlagiid theropods and paleognath birds. Front Earth Sc-Switz. 2021;9:662167.
80. Wu Q, Bailleul AM, Li ZH, O'Connor J, Zhou ZH. Osteohistology of the scapulocoracoid of and preliminary analysis of the shoulder joint in Aves. Front Earth Sc-Switz. 2021;9: 617124.
81. Kundrát M, Nudds J, Kear BP, Lü JC, Ahlberg P. The first specimen of *Archaeopteryx* from the Upper Jurassic Mörnsheim Formation of Germany. Hist Biol. 2019;31(1):3–63.
82. Nesbitt SJ, Turner AH, Spaulding M, Conrad JL, Norell MA. The theropod furcula. J Morphol. 2009;270(7):856–79.
83. Gauthier J. Saurischian monophyly and the origin of birds. Mem Calif Acad Sci. 1986;8:1–55.
84. Ostrom JH. *Archeopteryx* and origin of birds. Biol J Linn Soc. 1976;8(2):91–182.
85. Ruben J. Reptilian physiology and the flight capacity of *Archaeopteryx*. Evolution. 1991;45(1):1–17.
86. Benson RBJ, Choiniere JN. Rates of dinosaur limb evolution provide evidence for exceptional radiation in Mesozoic birds. P Roy Soc B: Biol Sci. 2013;280(1768):20131780.
87. Middleton KM, Gatesy SM. Theropod forelimb design and evolution. Zool J Linn Soc. 2000;128(2):149–87.
88. Chiappe L, Norell M, Clark J. Phylogenetic position of Mononykus (Aves: Alvarezsauridae) from the Late Cretaceous of the Gobi desert. Memoirs-Queensland Museum. 1996;39:557–82.
89. Xu X, Wang X. A new dromaeosaur (Dinosauria : Theropod) from the Early Cretaceous Yixian Formation of western Liaoning. Vert PalAs. 2004;43(02):111–9.
90. Xu X, Zhao Q, Norell M, Sullivan C, Hone D, Erickson G, Wang XL, Han FL, Guo Y. A new feathered maniraptoran dinosaur fossil that fills a morphological gap in avian origin. Chinese Sci Bull. 2009;54(3):430–5.
91. Han G, Chiappe LM, Ji SA, Habib M, Turner AH, Chinsamy A, Liu XL, Han LZ. A new raptorial dinosaur with exceptionally long feathering provides insights into dromaeosaurid flight performance. Nat Commun. 2014;5:5.
92. Barta DE, Nesbitt SJ, Norell MA. The evolution of the manus of early theropod dinosaurs is characterized by high inter- and intraspecific variation. J Anat. 2018;232(1):80–104.
93. Ostrom JH. A new theropod dinosaur from the Lower Cretaceous of Montana. Postilla. 1969;128:1–17.
94. Norell MA, Makovicky PJ. Dromaeosauridae. In: Weishampel DB, Dodson P, Osmólska H, editors. The Dinosauria. 2nd ed. Oakland: University of California Press; 2004. p. 196–209.
95. Hendrickx C, Bell PR, Pittman M, Milner ARC, Cuesta E, O'Connor J, Loewen M, Currie PJ, Mateus O, Kaye TG, Delcourt R. Morphology and distribution of scales, dermal ossifications, and other non-feather integumentary structures in non-avialan theropod dinosaurs. Biol Rev. 2022;97(3):960–1004.
96. Hieronymus TL. Flight feather attachment in rock pigeons (*Columba livia*): covert feathers and smooth muscle coordinate a morphing wing. J Anat. 2016;229(5):631–56.
97. Navalón G, Marugán-Lobón J, Chiappe LM, Luis Sanz J, Buscalioni ÁD. Soft-tissue and dermal arrangement in the wing of an Early Cretaceous bird: Implications for the evolution of avian flight. Sci Rep-Uk. 2015;5(1):14864.
98. Jenni L, Ganz K, Milanesi P, Winkler R. Determinants and constraints of feather growth. PLoS ONE. 2020;15(4): e0231925.
99. Goel MD, Rawat U. Design and analysis of wing structures of micro air vehicles. Procedia Engineer. 2017;173:1602–10.
100. Alerstam T, Rosén M, Bäckman J, Ericson PGP, Hellgren O. Flight speeds among bird species: allometric and phylogenetic effects. Plos Biol. 2007;5(8): e197.
101. Sievwright H, Macleod N. Eigensurface analysis, ecology, and modelling of morphological adaptation in the falconiform humerus (Falconiformes: Aves). Zool J Linn Soc. 2012;165(2):390–419.
102. Bribiesca-Contreras F, Parslew B, Sellers WI. A quantitative and comparative analysis of the muscle architecture of the forelimb myology of diurnal birds of prey (Order Accipitriformes and Falconiformes). Anat Rec. 2019;302(10):1808–23.
103. O'Connor J, Zhou ZH, Xu X. Additional specimen of Microraptor provides unique evidence of dinosaurs preying on birds. P Natl Acad Sci USA. 2011;108(49):19662–5.
104. O'Connor J, Zheng X, Dong L, Wang X, Wang Y, Zhang X, Zhou Z. Microraptor with ingested lizard suggests non-specialized digestive function. Curr Biol. 2019;29(14):2423–9.e2.
105. Hone DWE, Alexander Dececchi T, Sullivan C, Xing X, Larsson HCE. Generalist diet of *Microraptor zhaoianus* included mammals. J Vertebr Paleontol. 2022;42(2): e2144337.
106. Peregrine falcon. National wildlife federation: Merrifield, VA; 2024. https://www.nwf.org/Educational-Resources/Wildlife-Guide/Birds/Peregrine-Falcon. Accessed 31 May 2024.
107. Fargallo JA, Navarro-López J, Cantalapiedra JL, Pelegrin JS, Hernández FM. Trophic niche breadth of Falconidae species predicts biomic specialisation but not range size. Biology. 2022;11(4):522.
108. Greenewalt CH. Dimensional relationships for flying animals. Smithson Misc Collect. 1962;144(2):1–46.
109. Hartman FA. Locomotor mechanisms of birds. Smithson Misc Collect. 1961;143(1):1–91.
110. Durmus S. Theoretical model proposal on direct calculation of wetted area and maximum lift-to-drag ratio. Aircr Eng Aerosp Tech. 2021;93(6):1097–103.
111. Zhou Z. The Jehol Biota, an Early Cretaceous terrestrial Lagerstätte: new discoveries and implications. Natl Sci Rev. 2014;1(4):543–59.
112. Zhou ZH, Zhang FC. Anatomy of the primitive bird Sapeornis chaoyangensis from the Early Cretaceous of Liaoning, China. Can J Earth Sci. 2003;40(5):731–47.
113. Wang M, O'Connor JK, Bailleul AM, Li Z. Evolution and distribution of medullary bone: evidence from a new Early Cretaceous enantiornithine bird. Natl Sci Rev. 2020;7(6):1068–78.
114. Zhou ZH, Zhang FC. Two new ornithurine birds from the Early Cretaceous of western Liaoning, China. Chin Sci Bull. 2001;46(15):1258–64.
115. Habib MB, Ruff CB. The effects of locomotion on the structural characteristics of avian limb bones. Zool J Linn Soc. 2008;153(3):601–24.
116. Lee S, Thomas JW. *(Invited)* Humeral bone strength and flight in eumaniraptoran dinosaurs. ECS Tran. 2021;104(12):3.
117. Meyers RA. Morphology of the shoulder musculature of the American kestrel, *Falco sparverius* (Aves), with implications for gliding flight. Zoomorphology. 1992;112(2):91–103.
118. Cobb SE, Sellers WI. Inferring lifestyle for Aves and Theropoda: a model based on curvatures of extant avian ungual bones. Plos One. 2020;15(2):e0211173.
119. Burnham DA, Feduccia A, Martin LD, Falk AR. Tree climbing–a fundamental avian adaptation. J Syst Palaeontol. 2011;9(1):103–7.
120. Lautenschlager S. Morphological and functional diversity in therizinosaur claws and the implications for theropod claw evolution. P Roy Soc B: Biol Sci. 2014;281(1785):20140497.
121. Birn-Jeffery AV, Miller CE, Naish D, Rayfield EJ, Hone DWE. Pedal claw curvature in birds, lizards and mesozoic dinosaurs – complicated categories and compensating for mass-specific and phylogenetic control. PLoS ONE. 2012;7(12): e50555.
122. Dececchi TA, Larsson HCE. Assessing arboreal adaptations of bird antecedents: testing the ecological setting of the origin of the avian flight stroke. PLoS ONE. 2011;6(8): e22292.
123. Nations JA, Heaney LR, Demos TC, Achmadi AS, Rowe KC, Esselstyn JA. A simple skeletal measurement effectively predicts climbing behaviour in a diverse clade of small mammals. Biol J Linn Soc. 2019;128(2):323–36.

124. Kirk EC, Lemelin P, Hamrick MW, Boyer DM, Bloch JI. Intrinsic hand proportions of euarchontans and other mammals: implications for the locomotor behavior of plesiadapiforms. J Hum Evol. 2008;55(2):278–99.
125. Lemelin P. Morphological correlates of substrate use in didelphid marsupials: implications for primate origins. J Zool. 1999;247(2):165–75.
126. Manning PL, Margetts L, Johnson MR, Withers PJ, Sellers WI, Falkingham PL, Mummery PM, Barrett PM, Raymont DR. Biomechanics of dromaeosaurid dinosaur claws: application of X-ray microtomography, nanoindentation, and finite element analysis. Anat Rec. 2009;292(9):1397–405.
127. Sullivan C, Hone DWE, Xu X, Zhang FC. The asymmetry of the carpal joint and the evolution of wing folding in maniraptoran theropod dinosaurs. P Roy Soc B-Biol Sci. 2010;277(1690):2027–33.
128. Paul GS. Dinosaurs of the air: the evolution and loss of flight in dinosaurs and birds. Baltimore: JHU Press; 2002.
129. Senter P. Comparison of forelimb function between *Deinonychus* and *Bambiraptor* (Theropoda: Dromaeosauridae). J Vertebr Paleontol. 2006;26(4):897–906.
130. Bachmann T, Emmerlich J, Baumgartner W, Schneider JM, Wagner H. Flexural stiffness of feather shafts: geometry rules over material properties. J Exp Biol. 2012;215(3):405–15.
131. Zheng X, O'Connor JK, Wang X, Pan Y, Wang Y, Wang M, Zhou Z. Exceptional preservation of soft tissue in a new specimen of *Eoconfuciusornis* and its biological implications. Natl Sci Rev. 2017;4(3):441–52.
132. Brown RE, Cogley AC. Contributions of the propatagium to avian flight. J Exp Zool. 1996;276(2):112–24.
133. Serrano FJ, Chiappe LM. Aerodynamic modelling of a Cretaceous bird reveals thermal soaring capabilities during early avian evolution. J R Soc Interface. 2017;14(132):20170182.
134. Pennycuick CJ. Modelling the flying bird. 1st ed. Burlington: Elsevier; 2008.
135. Butler PJ. The physiological basis of bird flight. Philos Trans R Soc B Biol Sci. 2016;371(1704):20150384.
136. Novas FE, Agnolin F, Brissón Egli F, Lo Coco GE. Pectoral girdle morphology in early-diverging paravians and living ratites: implications for the origin of flight. B Am Mus Nat Hist. 2020;440:345–53.
137. Voeten DFAE, Cubo J, de Margerie E, Röper M, Beyrand V, Bureš S, Tafforeau P, Sanchez S. Wing bone geometry reveals active flight in *Archaeopteryx*. Nat Commun. 2018;9(1):923.
138. Heers AM, Varghese SL, Hatier LK, Cabrera JJ. Multiple functional solutions during flightless to flight-capable transitions. Front ecol evol. 2021;8:8.
139. Wang S, Ma Y, Wu Q, Wang M, Hu D, Sullivan C, Xu X. Digital restoration of the pectoral girdles of two Early Cretaceous birds and implications for early-flight evolution. Elife. 2022;11: e76086.
140. Mayr G. The coracoscapular joint of neornithine birds—extensive homoplasy in a widely neglected articular surface of the avian pectoral girdle and its possible functional correlates. Zoomorphology. 2021;140(2):217–28.
141. Hu D, Xing X, Lianhai H, Sullivan C. A new enantiornithine bird from the Lower Cretaceous of western Liaoning, China, and its implications for early avian evolution. J Vertebr Paleontol. 2012;32(3):639–45.
142. Ksepka DT. Evolution of birds. In: Scanes CG, Dridi S, editors. Sturkie's avian physiology. 7th ed. San Diego: Academic Press; 2022. p. 83-107.
143. Vazquez RJ. Functional osteology of the avian wrist and the evolution of flapping flight. J Morphol. 1992;211(3):259–68.
144. Feneck EM, Bickley SRB, Logan MPO. Embryonic development of the avian sternum and its morphological adaptations for optimizing locomotion. Diversity. 2021;13(10):481.
145. Benton MJ. The birds. Vertebrate palaeontology. 4th ed: John Wiley & Sons, Ldt; 2015. p. 274-317.
146. Panyutina AA, Korzun LP, Kuznetsov AN. Forelimb Morphology of Bats. In: Panyutina AA, Korzun LP, Kuznetsov AN, editors. Flight of mammals: from terrestrial limbs to wings. Cham: Springer International Publishing; 2015. p. 115–203.
147. McCracken GF, Safi K, Kunz TH, Dechmann DKN, Swartz SM, Wikelski M. Airplane tracking documents the fastest flight speeds recorded for bats. R Soc Open Sci. 2016;3(11): 160398.
148. Hefler C, Ying W, Grosmougin M, Chotard M, Pittman M. Unsteady aerodynamic features and wing-wing interactions in Microraptor flight. Society of vertebrate paleontology 83rd annual meeting. 2023. p. 209.
149. Wang X, McGowan AJ, Dyke GJ. Avian wing proportions and flight styles: first step towards predicting the flight modes of Mesozoic birds. PLoS ONE. 2011;6(12): e28672.
150. Simmons NB, Seymour KL, Habersetzer J, Gunnell GF. Primitive Early Eocene bat from Wyoming and the evolution of flight and echolocation. Nature. 2008;451(7180):818–21.
151. Akeda T, Fujiwara SI. Coracoid strength as an indicator of wing-beat propulsion in birds. J Anat. 2023;242(3):436–46.
152. Lee S-I, Kim J, Park H, Jabłoński PG, Choi H. The function of the alula in avian flight. Sci Rep-Uk. 2015;5(1):9914.
153. Bao H, Song B, Yang W, Xue D. The function of the alula with different geometric parameters on the flapping wing. Phys Fluids. 2021;33(10): 101907.
154. Ksepka DT. Feathered dinosaurs. Curr Biol. 2020;30(22):R1347–53.
155. Amador LI, Simmons NB, Giannini NP. Aerodynamic reconstruction of the primitive fossil bat *Onychonycteris finneyi* (Mammalia: Chiroptera). Biol Lett. 2019;15(3):20180857.
156. McGuire JA. Allometric prediction of locomotor performance: an example from southeast asian flying lizards. Am Nat. 2003;161(2):337–49.
157. Socha JJ, Jafari F, Munk Y, Byrnes G. How animals glide: from trajectory to morphology. Can J Zool. 2015;93(12):901–24.
158. Xu L, Wang M, Chen R, Dong L, Lin M, Xu X, Tang J, You H, Zhou G, Wang L, He W, Li Y, Zhang C, Zhou Z. A new avialan theropod from an emerging Jurassic terrestrial fauna. Nature. 2023;621(7978):336–43.
159. Xu X, Zhou HH, Prum RO. Branched integumental structures in *Sinornithosaurus* and the origin of feathers. Nature. 2001;410(6825):200–4.
160. Colbert EH, Russell DA, Matthew WD, Brown B. The small Cretaceous dinosaur *Dromaeosaurus*. Am Mus Novit. 1969;1969(2380):1–49.
161. Perle A, Norell MA, Clark JM. A new maniraptoran theropod, *Achillobator giganticus* (Dromaeosauridae), from the Upper Cretaceous of Burkhant, Mongolia. Contrib Dept Geol Natl Univ Mongolia. 1999;101:1.
162. Burnham DA, Derstler KL, Currie PJ, Bakker RT, Zhou Z, Ostrom JH. Remarkable new birdlike dinosaur (Theropoda: Maniraptora) from the Upper Cretaceous of Montana. Univ Kansas Paleontol. 2000;13:1–14.

Publisher's Note